ELSEVIER

Computational Materials Science 12 (1998) 157–191

COMPUTATIONAL MATERIALS SCIENCE

Order-*N* tight-binding methods for electronic-structure and molecular dynamics

Pablo Ordejón [1]

Departamento de Física, Universidad de Oviedo, 33007 Oviedo, Spain

Accepted 15 June 1998

Abstract

During the last few years, there has been an intense effort in the development of the so-called Order-*N* methods to solve the electronic-structure problem, for which the numerical efforts scale only linearly with the size of the system. The combination of these algorithms with total energy schemes has expanded our capability of performing electronic-structure based molecular dynamics (MD) simulations for systems of unprecedented size. In general, Order-*N* methods yield approximate solutions, based on physically motivated approximations. The central idea is, in most cases, the concept of localization (or the dependence of the relevant physical quantities on *only* the local environment). Therefore, the Tight-Binding (TB) formulation (or, more generally, the use of some kind of localized basis set), either from first principles or in an empirical form, is a natural framework to develop and apply Order-*N* schemes. In this paper we analyze the main ideas involved in these methods and their different implementations. We will focus on schemes to compute total energies and forces, therefore suited for MD simulations, and also on approaches to study the spectral properties like the density of states and eigenvalue information. These two classes of methods provided valuable complementary information and are often based on very similar assumptions and formalisms.

1. Introduction

Since the early days of quantum mechanics, the prospect of being able to predict and explain the behavior of condensed matter systems at the atomic level, by solving the fundamental equations for the nuclei and electrons, has fascinated many generations of scientists. Over the years, this has proven to be an exceedingly difficult task, because of the intrinsic complexity of the solution of the coupled many-body quantum-mechanical problem, and the tremendous numerical workload involved even for approximate solutions. However, atomic, molecular and solid state physics, quantum chemistry, materials science, and many other disciplines have contributed in the search of viable ways to put this prospect to practice, both in the derivation of approximate theories to simplify the original many-body problem and in the development of computational methods to solve these theories for particular systems. At the same time, the available computing power provided by digital computers has grown by several orders of magnitude over the last three decades, allowing the application of these techniques to real problems.

The application of quantum-mechanical computations to the study of atomistic processes in

[1] Supported by Spain's DGES Grant PB95-0202 and by a Motorola Phoenix Corporate Research Laboratories Sponsored Research Project.

0927-0256/98/$00.00
PII S0927-0256(98)00027-5

condensed matter has blossomed during the last two decades due of the combination of those two factors. Nowadays, calculations of structural, energetic and even dynamical properties of atomic systems of *moderate* size can be done routinely, and are an important piece of our understanding of the microscopic processes in condensed matter. These calculations can provide a wealth of information that is not easily or possibly accessible in experiments, and therefore are of great importance in fields like materials science, biochemistry, solid state physics, etc. The everyday necessity of treating larger systems is present in all these applications: the problems of technological relevance in materials and biophysics usually involve thousands or even millions of atoms.

Most of the methods currently used in atomistic calculations rely on the Born–Oppenheimer approximation, and therefore treat ions as classical particles that move in the potential produced by the quantum-mechanical electrons. The electronic-structure problem is therefore the bottleneck that limits the size and complexity of the systems that can currently be tackled. Different electronic-structure methods present different computational requirements. However, a common feature of the traditional methods is the over-linear scaling of the computational effort (CPU time and memory) with the number of atoms or electrons N_e in the system. This scaling ranges from exponential for the Configuration Interaction methods of quantum chemistry (QC) to a power law in one-electron theories like Density Functional Theory [1] (DFT) and Hartree–Fock (HF). This nonlinear scaling represents a serious limiting factor in the size of the systems that can be approached in practice. In the case of the one-electron theories (to which we will restrict ourselves in this paper), the unfavorable scaling is a consequence of the Pauli exclusion principle between electrons. This is usually expressed in terms of *global* orthonormalization conditions for the one-electron states, or idempotency constraints for the density matrix (DM), both of which would scale as, at least, $\mathcal{O}(N_e^2)$. For instance, the traditional direct diagonalization scheme, in which all the Hamiltonian eigenstates are computed, scales as $\mathcal{O}(N_b^3)$ (where N_b is the size of the basis set, which is in general proportional to the number of electrons N_e).

An important step towards larger system sizes was taken by Car and Parrinello [2], who initiated a new set of methods [3] for which the numerical effort was largely diminished compared to methods of the time, improving the efficiency of large-scale electronic-structure calculations. These are iterative diagonalization techniques, in which the total energy is written as a functional of the *occupied* electronic wave functions, which are iterated toward the minimum energy solution. The required effort grows as $\mathcal{O}(N_e^2 N_b)$, which can be considerably less than that for direct diagonalization, specially if the number of basis orbitals per electron is large. Whereas for tight-binding (TB) Hamiltonians [4] the gain is not very large due to the small number of basis functions per electron, the impact on plane wave (PW) calculations has been enormous, because in this case the ratio between N_b and N_e is typically about 100. These methods have boosted the applicability of electronic-structure calculations, especially for first principles molecular dynamics (MD) applications. However, despite its tremendous importance, this class of methods still scales as the cube of the number of electrons for the CPU time, and the square for the memory. Due to this over-linear scaling the application of electronic-structure methods is limited to systems with a few hundred electrons in the case of first-principle methods and less that a thousand for empirical tight-binding (ETB) Hamiltonians (using the most powerful computational platforms).

On the other hand, since many years there is abundant evidence that this nonlinear scaling of the electronic-structure problem can be overcome. Although quantum mechanics requires that the properties cannot be purely local, the effect of the surrounding decays rapidly (in a sense that will be discussed in the next few sections). Particularly Heine and coworkers [5] have emphasized that the local properties of a region can be computed from the knowledge of the electronic states only in the vicinity of that region. Kohn [6] has recently reformulated this "nearsightedness" principle in a more precise manner. The recursion method is one of the techniques that has used these ideas to compute *local* properties of large systems with an effort

independent of the size of the system. This naturally leads to linear scaling or Order-N algorithms, since different parts can be computed independently, with an effort independent of the system size.

In the last few years, there has been a renewed awareness of the possibility of linear scaling electronic-structure methods. As a result, many Order-N methods have been proposed and applied in different contexts and systems. These developments have expanded the applicability of electronic-structure calculations to systems of unprecedented size, to the point that we can now treat, at the ab-initio level, system sizes that were hardly manageable with empirical methods only a few years ago. We will refer to this set of methods as "modern" Order-N methods. These are characterized by the aim towards being able to perform MD simulations, relaxations, etc., and therefore total energies and forces are required. The solution of the whole system, and not only local information, is then needed.

It is important to stress here that all the Order-N methods in which the properties of the *whole* system are computed (for instance, the charge distribution, the total energy or the forces on all atoms), provide necessarily *approximations* to the exact solution of the effective one-electron Hamiltonian. These approximations are based on physical assumptions, which are generally connected to the above mentioned locality or nearsightedness principle in one way or another. The details of the approximations are different for different schemes, as well as how to put them into practice.

The fact the some kind of localization is invoked in Order-N approaches has important consequences in determining the optimal basis sets for linear scaling algorithms. It is clear that *localized* bases will be preferred as a natural way to express localization conditions. For this reason, the use of extended basis sets like PW in the context of linear scaling has proven to be difficult (but not impossible [7]), and most of the Order-N methods have been developed either under the assumption of some kind of local orbitals basis, or directly in a real space representation. This makes ETB models the ideal testing ground for development and application of Order-N methods. There have been nevertheless several recent attempts to extend Order-N schemes to ab-initio calculations. These are generally reformulations of the first-principle theories in the form of a TB Hamiltonian, usually by the explicit use of localized, atomic-like basis sets, or by some other real space formalism through the use of intermediate "support functions" of localized orbital character. We will designate this general class of methods as ab-initio tight-binding (AITB) formulations. The advantage of ETB lies in its significantly reduced computational demands compared to ab-initio methods, since the construction of the Hamiltonian matrix is straightforward from the parametrization. In the AITB case, the Hamiltonian has first to be computed from first principles, and then solved to obtain the energy, charge distribution, etc., and both stages need scale linearly with the size of the system. The calculation of this Hamiltonian in Order-N operations is by no means a trivial problem, and much work has been devoted to it in the last few years [8–19]. However, the description of these methods is beyond the scope of this work, and here we will concentrate on the problem of how to solve a given Hamiltonian in Order-N operations.

The range of the linear scaling electronic-structure methods is quite large. However, they can be roughly divided in two broad classes, depending on the main physical quantities that the method is able to provide. The first class is aimed at the calculation of total energies and forces, and are therefore suited for MD simulations. The second one focuses on the spectral properties like densities of states, response functions and optical spectra. The border between these classes is, nevertheless, quite ill defined, and some methods can be applied for both tasks. In addition, some of the underlying techniques may be common to some of the methods belonging to the two classes. The rest of this paper is organized as follows. In Section 2 we describe the underlying physical principles which allow us to build Order-N schemes, and give an example of how to exploit them in a particular implementation. In Section 3 we describe a group of methods which are based on variational principles to calculate the energies and forces. In Section 4 a class of methods with the same aim of computing total energies and forces, but which are not varia-

tional, are introduced. In Section 5 we discuss methods that allow us to obtain information about the spectrum of the system in Order-N operations. Finally, we present our conclusions in Section 6.

2. Locality in electronic-structure

The central ideas behind most of the Order-N methods for electronic-structure exploit the concept of *locality*. It is known since many years that most of the static properties of many-electron systems at a certain position depend only on the local environment within a few shells of neighbors. Examples of this are the local density of states, charge distribution, local magnetic moments, binding energies, etc. The fact that the properties of bulk materials can be defined and calculated without any reference to the surface of the material (with the exception of effects due to surface charge distributions and the associated polarization fields) is another example of this concept. This means for instance that the description of the bulk is independent of the boundary conditions. Although this is commonly assumed in an implicit way, much work has also been involved in exploiting this in an explicit way. One example is the Green's functions approach to the calculation of electronic states of surface [20] and in amorphous systems [21]. The recursion method [5,22] is the paradigm of a traditional electronic-structure method that exploits locality, and has been used very successfully in a variety of problems.

2.1. Nearsightedness principle

Regardless of the evident utility of locality, the concept remained vaguely defined until a precise statement was given very recently by Kohn [6], motivated by the development of modern Order-N techniques. Kohn has discussed a widely applicable principle of "nearsightedness" for equilibrium systems of many quantum-mechanical particles in an external potential $v(\mathbf{r})$. The formulation of the principle is that the physical properties of a part of a system are not affected by changes of the potential at distant regions, and is illustrated in Fig. 1. The principle states that, for $\mathscr{F}$ being a

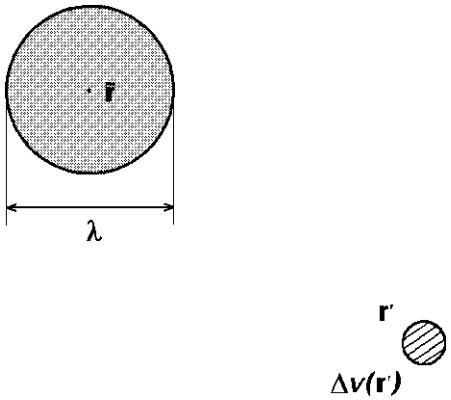

Fig. 1. Kohn's principle of nearsightedness for quantum many-particles systems: the static properties around $\bar{\mathbf{r}}$ do not depend on changes $\Delta v(\mathbf{r}')$ at distant regions.

static property depending on the coordinates within a volume ω of linear dimension λ around $\bar{\mathbf{r}}$, then, at constant chemical potential $\mu, \mathscr{F}$ is not sensitive to arbitrarily large changes in the potential $\Delta v(\mathbf{r}')$ if this change is restricted to distant positions $\mathbf{r}'$. Here λ is a typical de Broglie wavelength of the system which determines the degree of locality. It should be emphasized that the potential must remain unchanged in the region around $\bar{\mathbf{r}}$, and changes only in regions far compared with λ. Long range electric fields like those occurring in polar crystals or originating from surface charges in insulators should be treated separately in a self-consistent manner, but do not affect the basics of the principle.

As Kohn points out, nearsightedness implies immediately the possibility of existence of linear scaling methods. It would suffice to divide the system, of volume Ω, in subsystems of volumes of order $\omega_i \propto \lambda^3$. For each subsystem, we extract a volume ω_i' containing ω_i plus some buffer region around it. The procedure is sketched in Fig. 2. We then solve the properties of each volume ω_i' separately, using hard wall boundary conditions. If the volumes ω_i' are sufficiently larger than ω_i, then the properties within ω_i will be properly described because of nearsightedness. Therefore, computing the properties within *each* ω_i requires an effort independent of the size of the system (since it can be done using only information within

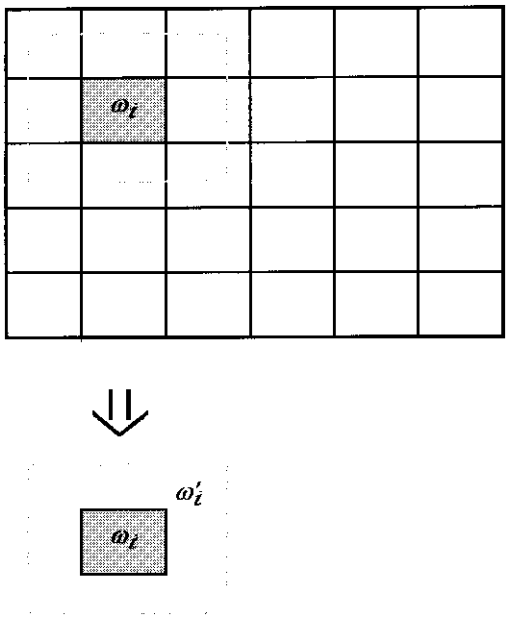

Fig. 2. The sketch of a procedure to obtain a linear scaling scheme. The system is split into subsystems of volume ω_i, and each one is independently solved, together with some buffer region, with hard wall boundary conditions.

ω_i'). Since the number of volumes ω_i will be proportional to the system size, computing the properties of the whole system will be an $\mathcal{O}(N)$ task. This general scheme is in fact very closely followed by one of the first modern linear scaling methods, as will be described in Section 2.4.

Locality in electronic-structure manifests in many ways as we have indicated. There are however two very well known facts which are related to locality and nearsightedness which play a role of paramount importance in the theory of solids and molecular systems in general, and in the development of Order-N methods in particular. These are the existence of localized Wannier-like functions and the decay of the DM at large distances.

2.2. Wannier functions

The fact that the properties of a system can be described either with extended eigenstates or, alternatively, with localized wave functions, is well known in solid state physics and in quantum chemistry. In crystalline solids these localized states are the Wannier functions [23], which are the basis of many theoretical developments like the semiclassical theory of electron dynamics [24]. In molecules or clusters, these correspond to the "localized molecular orbitals" of quantum chemistry [25]. In both cases, the localized states are just a unitary transformation of the corresponding extended eigenstates (Bloch functions for solids and canonical molecular orbitals in molecules). For the purpose of computing ground state properties, only the occupied part of the spectrum is usually required, so that the localized states are a unitary transformation of the *occupied* eigenfunctions. (Note that in some cases, as in the calculation of electronic correlation in many-body approaches, empty states are also needed, in which case one can also define localized functions spanning the empty subspace.)

The decay of the Wannier functions has been the subject of many investigations, following early work of Kohn [26], who probed that, for an isolated band in a 1-D crystal with inversion symmetry, the Wannier functions decay exponentially for a system with a gap, and only as a power law for a metal. In the insulator case, he further showed that the exponent of the decay is related the band gap, so that a larger gap implies a faster decay. Although much work has been done, a general proof for 3-D crystals with composite bands (i.e., a group of bands that are degenerate at some point of the Brillouin zone) is still missing. Nevertheless, there is evidence that exponential localization is a general property of insulators, even for systems with no periodicity (like clusters, disordered solids, defects or surfaces). We will refer to these localized functions in nonperiodic systems as generalized Wannier functions (GWF). The interested reader can find details in an excellent review of the current status of the issue, in the context of a method to obtain maximally localized Wannier functions, by Marzari and Vanderbilt in Ref. [27].

2.3. Density matrix

Another manifestation of locality in electronic-structure is the decay of the DM in real space. For a system with $N = N_e/2$ electrons of each spin (we will assume unpolarized systems throughout the

paper; generalization to spin-polarized systems is straightforward in most cases) the density operator is defined as

$$\hat{\rho} = 2\hat{F}_\beta = 2F_\beta(\hat{H}) = 2\sum_i^{N_b} F_\beta(\epsilon_i)|\psi_i\rangle\langle\psi_i|, \tag{1}$$

where

$$F_\beta(E) = [e^{\beta(E-\mu)} + 1]^{-1} \tag{2}$$

is the Fermi–Dirac projection operator at temperature $T(\beta = 1/kT)$, μ, the chemical potential and N_b, the basis set size, or the number of orbitals in the system. The second representation, in terms of the eigenstates of the Hamiltonian ψ_i makes explicit the projection character of the density operator. The real space representation is readily obtained as

$$\rho(\mathbf{r},\mathbf{r}') = 2\sum_i^{N_b} F_\beta(\epsilon_i)\psi_i^*(\mathbf{r})\psi_i(\mathbf{r}'). \tag{3}$$

The localization properties of the DM for $T = 0$ are easily verified with the following argument. At zero temperature, the Fermi function is just the step function, so that Eq. (1) can be expressed as a projection onto the occupied space

$$\hat{\rho} = 2\sum_i^{N} |\psi_i\rangle\langle\psi_i|. \tag{4}$$

Note that the sum runs only to the N lowest energy orbitals. This projection can be computed using the occupied eigenstates or any other set of functions spanning the same occupied space (i.e., any unitary transformation of the occupied eigenstates). One possible choice is to use the GWF $|\chi_i\rangle$ introduced above, instead of the eigenstates $|\psi_i\rangle$. In this representation, the real space DM is given by

$$\rho(\mathbf{r},\mathbf{r}') = 2\sum_i^{N} \chi_i^*(\mathbf{r})\chi_i(\mathbf{r}'). \tag{5}$$

Since the GWF are localized, $\rho(\mathbf{r},\mathbf{r}')$ will also decay with the distance $|\mathbf{r}-\mathbf{r}'|$, exponentially for insulators and with a power law in metals, as dictated by the behavior of the GWF. For the case of a periodic insulator in 1-D with an energy gap $\delta\epsilon$, the decay was shown by Kohn [26] to be exponential, with a spatial range proportional to $\delta\epsilon^{-1/2}$. For metals, the power law decay follows from the behavior of the GWF. In the simple case of the free electron 3-D jellium model, the decay of the density matrix is known analytically. It depends only on the modulus of the distance $s = |\mathbf{r}-\mathbf{r}'|$, as

$$\rho(s) = \frac{4\pi}{s^3}(\sin(k_F s) - (k_F s)\cos(k_F s)), \tag{6}$$

where k_F is the Fermi vector. The slow (power law) oscillatory decay is due to the discontinuity of the Fermi–Dirac distribution (step function) in reciprocal space.

The decay rate of the DM in real space is even more pronounced when the temperature is finite. In this case, even metals show exponential localization. For the free electrons case, this can be understood because the Fermi–Dirac function is no longer discontinuous in reciprocal space. Goedecker [28] has recently given an approximate analytical form for the decay in the free electron case for finite temperature, showing that, at large distances, the DM decays as $\exp(-c(k_B T/k_F)s)$, where $c = 1+\sqrt{2}$ and k_B is the Boltzmann constant. It is clear that for metals the localization will be stronger for higher temperatures. However, we must note that the localization is noticeably stronger than for $T = 0$ only when temperatures of the order of eV are reached, much higher than physical ionic temperatures. For systems with an energy gap between occupied and empty states, the effect of the temperature is much smaller than for metals, since the DM is already exponentially localized at $T = 0$. A noticeable change will only occur when the electronic temperature is comparable to the energy gap $\delta\epsilon$.

A general analysis of the DM decay for insulators and metals was presented by Baer and Head-Gordon [29,30]. The estimates are done on the basis of a Chebyshev expansion of the DM, as will be described in Section 4.1. They have shown how the range of the DM depends on the physical parameters like energy gap $\delta\epsilon$, temperature, etc. $W(\rho)$ is defined as the spatial range at which the value of $\rho(\mathbf{r},\mathbf{r}')$ may be neglected, to an accuracy of 10^{-D}. For insulators, the predicted behavior is

$$W(\rho) \approx \sqrt{\frac{\hbar^2}{4m_e\delta\epsilon}3D(D-1)}, \tag{7}$$

whereas for metals at finite temperature the estimate is

$$W(\rho) \approx \sqrt{\frac{\hbar^2}{3m_e\delta\epsilon}(D-1)\beta}. \tag{8}$$

Very recently, Ismail-Beigi and Arias [31] have also studied the decay of the DM in periodic potentials in arbitrary dimensions. Using analytical and scaling techniques, they have determined the coefficient γ of the exponential decay of the DM ($\rho(s) \sim \exp(-\gamma s)$) in some limits. For insulators at $T=0$, they find that, for the TB limit (large band gap $\delta\epsilon$ compared to the band width), $\gamma \propto \sqrt{\delta\epsilon}$, in agreement with previous results. However, for the weak binding limit (small band gap $\delta\epsilon$, compared to the band width), they find that the decay behaves as $\gamma \propto \delta\epsilon$. They argue that the case of typical semiconductors falls into this second category. For metals, they find a different behavior for high and low temperatures. For $T \to \infty$, they recover the $\gamma \propto \sqrt{T}$ described above by Baer and Head-Gordon. However, for $T \to 0$, the decay is like the one found by Goedecker in the free electron case: $\gamma \propto T/k_F$.

2.4. Divide and conquer approach

The first proposal of 'modern' linear scaling scheme was done by Yang in the beginning of the decade, with the "divide and conquer" (D&C) method [32,33]. The procedure is very similar to the one sketched in the discussion of the nearsightedness principle (Fig. 2). The idea is very appealing, since it provides a description of a large system in terms of its constituent parts (chemical bonds, functional groups, fragments, etc.). The D&C method was originally developed in the context of Density Functional Theory, although it was later extended to HF semiempirical QC Hamiltonians [34,35]. The method can also be applied to empirical TB Hamiltonians in a straightforward manner.

The D&C method intends to describe the charge distribution of the system in terms of contributions from the different fragments. Each fragment or subsystem has a supplementary buffer region, to help reduce truncation effects as shown in Fig. 2. It should be noted here that Dixon and Merz [34] have proposed a modification of the D&C scheme, in which the subsystems overlap with each other (besides having a buffer region, as in the scheme of Yang). The presence of overlapping regions seems to provide a better convergence, since it facilitates the propagation of information among subsystems.

In the first few formulations of the D&C method [32], the basic variable was the electron density (the diagonal terms of the density operator in real space: $n(r) = \rho(r,r)$), in the context of DFT. However, later formulations work with the representation of the DM in the atomic orbitals basis. This formulation is more general, since it permits the application of the method to several one electron Hamiltonians (DFT, HF, semiempirical methods and empirical TB). Therefore, we will present here the DM formulation.

The total energy takes different expressions depending on the one-electron Hamiltonian. However, it can usually be expressed in the general form

$$E = E_{BS} - E_{DC}, \tag{9}$$

where E_{BS} is the band structure energy

$$E_{BS} = 2\,\mathrm{Tr}(\hat{\rho}\hat{H}) = 2\sum_{i=1}^{N_b} F_\beta(\epsilon_i)\epsilon_i, \tag{10}$$

which is just the sum of the eigenvalues of the one-electron effective Hamiltonian $\hat{H}$ multiplied by the Fermi–Dirac occupations (the factor 2 is for spin). In the case of DFT, $\hat{H}$ is the Kohn–Sham Hamiltonian, whereas for HF, it is the Fock operator $\hat{F}$. The second term is a double-counting correction, which can also be obtained with the knowledge of the DM elements [32,34]. In ETB, the electronic energy would be just E_{BS}. Throughout this work we will only consider the band structure term. Inclusion of the double counting, when necessary, is straightforward.

A traditional solution to the total energy problem would be to solve the generalized eigenvalue problem for the whole system in order to obtain

the eigenvalues and calculate E_{BS} by means of Eq. (10). In the linear combination of atomic orbitals (LCAO) approximation, common to all TB schemes, the eigenstates are expressed as linear combinations of the basis functions $|\phi_\mu\rangle$

$$|\psi_i\rangle = \sum_{\mu=1}^{N_b} C_{\mu i}|\phi_\mu\rangle. \tag{11}$$

The eigenvalue problem reads

$$\mathbf{H}C_i = \mathbf{S}C_i\epsilon_i, \tag{12}$$

where $\mathbf{H}$ and $\mathbf{S}$ are the Hamiltonian and overlap matrices in the orbitals basis. An important observation is that Eq. (10) can be expressed in terms of the DM elements in the orbitals basis

$$E_{BS} = \sum_{\mu,v=1}^{N_b} \rho^{\mu v} H_{v\mu} \tag{13}$$

with

$$\rho^{\mu v} = \langle\phi^\mu|\hat{\rho}|\phi^v\rangle = 2\sum_{i=1}^{N_b} F_\beta(\epsilon_i) C_{\mu i} C_{vi}. \tag{14}$$

(Here we have introduced $\{\phi^\mu\}$, the dual basis of $\{\phi_\mu\}$, which is given by $\phi^\mu = \sum_v S^{-1}_{\mu v}\phi_v$, satisfying $\langle\phi^\mu|\phi_v\rangle = \delta_{\mu v}$ and $\sum_\mu |\varphi^\mu\rangle\langle\phi_\mu| = \hat{I}$; the dual basis and with a tensor representation of operators [36] allows us to work with nonorthogonal bases; for orthogonal bases, the dual is just the original one, and the usual formulation is recovered). This direct approach requires the solution of the eigenvalue problem for the complete system, which scales as N_b^3.

The D&C method provides an alternative to this cubic scaling. The system is split into subsystems, as previously discussed. Each of this subsystems (including its buffer region) is solved independently. For subsystem α, an eigenvalue problem is set up in terms of the Hamiltonian $\mathbf{H}^\alpha$ and overlap $\mathbf{S}^\alpha$ matrices between pairs of basis function *within* subsystem α and its buffer

$$\mathbf{H}^\alpha C_i^\alpha = \mathbf{S}^\alpha C_i^\alpha \epsilon_i^\alpha. \tag{15}$$

Note that the size of these matrices is $(N_\alpha \times N_\alpha)$, where N_α is the number of basis orbitals within subsystem α and its buffer, much smaller than the total number of basis functions N_b. Therefore, the solution of Eq. (15) takes an effort of the order N_b^3, independent of the size of the system. In order to compute the total energy, we need the DM for the whole system, which has to be expressed as a sum of contributions from constituent subsystems. This is made possible by defining a partition matrix $\mathbf{p}_\alpha^{\mu v}$ for each subsystem, which satisfies the normalization condition

$$\sum_\alpha \mathbf{p}_\alpha^{\mu v} = 1 \tag{16}$$

for all μ, v. The system DM can be divided into subsystem contributions according to

$$\rho^{\mu v} = \sum_\alpha \mathbf{p}_\alpha^{\mu v}\rho^{\mu v} = \sum_\alpha \rho_\alpha^{\mu v}. \tag{17}$$

The explicit form of the partition matrices depends on the scheme of partition of the system. In the case of nonoverlapping subsystems, a possible partition matrix is proposed by Lee et al. [35]

$$\mathbf{p}_\alpha^{\mu v} = \begin{cases} 0 & \text{if } \mu \in \text{buffer and } v \in \text{buffer}, \\ \frac{1}{2} & \text{if } \mu \in \alpha \text{ and } v \in \text{buffer} \quad (\text{or vice versa}), \\ 1 & \text{if } \mu \in \alpha \text{ and } v \in \alpha. \end{cases} \tag{18}$$

Dixon and Merz proposed a different form, applicable to the case in which the subsystems do overlap

$$\mathbf{p}_\alpha^{\mu v} = \begin{cases} 0 & \text{if } \mu \in \text{buffer or } v \in \text{buffer}, \\ 1/n_{\mu v} & \text{if } \mu \in \alpha \text{ and } v \in \alpha, \end{cases} \tag{19}$$

where $n_{\mu v}$ is the number of different subsystem in which both ϕ_μ and ϕ_v appear as nonbuffer orbitals. The partition functions allow us to make an approximation for the subsystem DM to construct the system DM by Eq. (17)

$$\rho_\alpha^{\mu v} = 2\mathbf{p}_\alpha^{\mu v}\sum_{i=1}^{N_\alpha} F_\beta(\epsilon_i^\alpha) C_{\mu i}^\alpha C_{vi}^\alpha. \tag{20}$$

Therefore, the DM of the system is built from the eigenstates of each subsystem. An important point here is that there is a common chemical potential μ for all the subsystems, entering in the Fermi–Dirac function F_β. This assures that information be shared between subsystems, and allows charge transfer between them. The value of the chemical potential is determined by the normalization condition

$$N = \sum_{\mu,\nu=1}^{N_b} \rho^{\mu\nu} S_{\nu\mu} \tag{21}$$

in a self-consistent manner, and the band structure energy is obtained by means of Eq. (13).

In general, the goal is to compute the ground state properties of the system at $T=0$, which would correspond to $\beta = \infty$, and the step function for the Fermi–Dirac distribution. In practice, however, this would lead to instabilities in the procedure to compute the chemical potential (Fermi level), and the calculations are done at a finite β. This yields some errors in the energy, which can be kept small if β is chosen to be large enough. In essence, $1/\beta$ should be at most of the order of the energy gap, so that the occupations are not significantly affected. For metals, however, the error will always be present, and the results will reflect the finite temperature used in the calculation. We will come back to this point in the next few paragraphs.

The D&C method has been tested and applied in a variety of systems, most of them molecules and clusters. Fig. 3 shows the case of a tetrapeptide (a 31 atoms linear backbone chain with four glycine residues; see figure 1 in Ref. [37]). The calculations were done by Yang [37] with the non-self-consistent, Harris functional version of DFT [38]. The chain was divided into 13 subsystems, each containing one of the C or N atoms in the backbone of the chain, and the O and H atoms bonded to it. The buffer regions contain from zero to five shells of neighbors to the atoms in the corresponding subsystem. The figure shows the difference of the total energy computed with D&C method and the exact diagonalization result with the same basis, as a function of the number of shells of neighbors included in the buffer regions. Three different atomic orbital bases of increasing quality were used in the calculation: a Single- ζ basis (a single radial function for each occupied orbital in the free atom), a Double-ζ basis (with two independent radial functions per shell), and a Double-ζ + Polarization basis (the Double-ζ orbitals, plus an extra single shell of $l_{occ}+1$ angular momentum, where l_{occ} is the angular momentum of the higher occupied orbital of the atom). Here, and in what follows, we denote these three types of bases as SZ, DZ and DZP. It can be seen that the convergence with the number of shells of neighbors is exponential in all cases, as we would expect from the above considerations on the locality of the DM. Similar results were obtained by Dixon and Merz in their study of polyglycine structures.

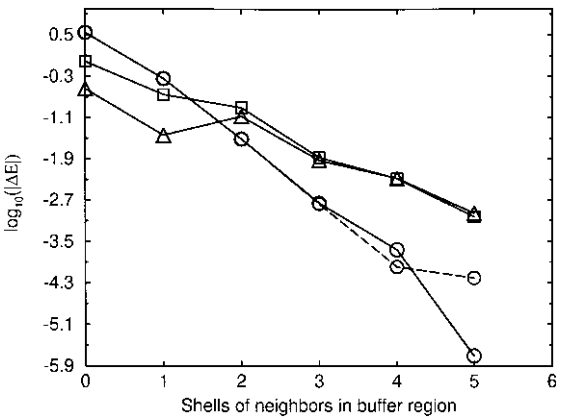

Fig. 3. Absolute value of errors in the total energies for a tetrapeptide molecule for the D&C approach, referred to the exact diagonalization result. Results for SZ, DZ and DZP bases are shown as circles, squares and triangles. Continuous lines are results obtained with an inverse temperature of $\beta = 100$ a.u., and broken lines for SZ correspond to $\beta = 200$ a.u.

A few comments on the results of the D&C method for molecules are in order. (i) The convergence to the diagonalization result is better for the smaller SZ basis set than for the more complete DZ and DZP. This fact can be due to two factors. First, the more delocalized character of the DZ and DZP bases, which contain orbitals with slowly decaying tails. Secondly, the smaller gap that results in the calculation with these larger bases, what would make the DM to decay more slowly. (ii) The calculations were done with $\beta = 100$ a.u., corresponding to a temperature of 3150 K. Fig. 3 also shows the results with the SZ basis, for $\beta = 200$ a.u., which show very little difference with the $\beta = 200$ a.u. results. The effect of the temperature is therefore very small, at least in this range of temperatures, for systems with relatively large energy gaps. (iii) The use of buffer functions in essential to obtain a good accuracy and minimize the truncation errors. The results with no buffer region show errors of the order of several a.u. that are not

acceptable. However, including just a first shell of neighbors reduces the deviation to values that are similar to the typical errors coming from the finite basis sets used. (iv) Results with different system sizes [37,39,34] indicate that, for the same kind of molecule, the buffer region size needed to achieve a given relative accuracy (energy per atom) is independent of the size of the molecule. Therefore, the calculation scales as $\mathcal{O}(N)$, since the number of the subsystems will be proportional to the number of atoms, and the size of the subsystems (including the buffer) does not increase with the system size. Examples of this linear scaling can be found in figure 4 of Ref. [34] and figure 2 of Ref. [35].

An important characteristic of the D&C approach is that it is not variational: the calculated total energy can be lower than the exact value. The exact energy is of course recovered when the subsystems cover the whole system. Despite the nonvariational character of the method, atomic forces can be computed as energy gradients, as demonstrated by Yang and coworkers [40,39]. They also show that, for linear molecules, the convergence of the forces with the number of atoms in the buffer regions is similar to that of the energy.

The application of the D&C method to solid-state problems has been scarce. Zhu et al. [41] generalized the method to crystalline systems, and tested it in a variety of solids with small unit cells, including metals, covalent semiconductors and insulators and ionic systems. The conclusions of these studies are similar to those reached in the molecular cases. The energies and structural properties of the crystals improve systematically with the use of buffer regions containing more shells of neighbors. However, since the systems are crystals in 3-D, the increase of the number of atoms with the number of shells is much larger than in the linear molecules, and the cost of the calculations increases at a higher rate. Note that the application of the D&C approach to solids is similar to an embedding calculation, in which a part of the solid is embedded in the buffer region to obtain its local properties. The energy and electronic-structure is computed locally, with no need to refer to reciprocal space or to k-point sampling in the calculation. This is a clear advantage if one wishes to study systems with broken periodicity, like defects, surfaces, or periodic cells with a very large number of atoms.

One of the conclusions of the work of Zhu et al. for crystals is that all the systems under consideration (regardless of the insulating or metallic character) show the same convergence properties as a function of the buffer size. This conclusion is reached based on the error of the total energies versus buffer size (see figures 1 and 4 of Ref. [41]). However, a weak point in the argument is that the reference energy used to compute the error is not the exact energy of the system, as would be obtained by a converged k-point sampling calculation in the unit cell with diagonalization. Zhu et al. use as a reference the energy obtained with the D&C method with a given, large number of shells of buffer atoms. Whereas for crystals with a gap this value is probably very close to the exact k-point sampling result, it can be significantly different for metallic cases like the lithium and copper crystals studied in Ref. [41]. Therefore, these convergence results should be taken with caution. In principle, and given the slower decay in the DM for metallic systems, we would expect the convergence with buffer regions to be slower in the case of metals. Another point to notice is that the calculations were done with a finite temperature (about 1000 K). This can also have a significant effect for the metallic cases, for which the Fermi surface is being smeared, thus making the DM more localized than the true $T=0$ DM. A detailed analysis of these effects, taking the correct reference energy and the correct zero temperature limit, would be very relevant to clarify the convergence properties of this method for metals and insulators.

3. Variational functional methods

An important class of Order-N methods follows the tradition of Car–Parrinello [2] or iterative minimization approaches [3]. In these, the electronic energy is expressed as a functional that is minimized in terms of the electronic variables. This method is particularly well suited for MD simulations, since the solution of previous time steps can be extrapolated to obtain an initial guess for the functional minimization in the current time step.

The cost of each MD step is therefore greatly reduced. Besides, since the calculation is variational, accurate forces are obtained as analytical derivatives of the energy functional, by means of the Hellman–Feynman theorem.

3.1. Conventional energy functionals

If we assume that the calculation is done at $T=0$, the electronic band structure energy can be expressed in terms of the DM like in Eq. (13), or equivalently as a trace of the Hamiltonian in the space of the *occupied* wave functions

$$E_{\mathrm{BS}} = 2\sum_{i=1}^{N}\langle\psi_i|\hat{H}|\psi_i\rangle. \tag{22}$$

Therefore, the energy functional can be expressed either in terms of the elements of the DM as in Eq. (13) or in terms of the occupied states as in Eq. (22). The ground state energy can therefore be computed minimizing the energy with respect to the values of either $\rho^{\mu\nu}$ or ψ_i, by virtue of the variational principle.

It should be noted here that functionals based on the orbital formulations have been the common choice in the context of PW calculations. In that case, the number of occupied states $N = N_{\mathrm{e}}/2$ is much smaller than the number of plane waves N_{b}. The computational cost is therefore reduced from $\mathcal{O}(N_{\mathrm{b}}^3)$ in standard diagonalization or in DM formulations to $\mathcal{O}(N_{\mathrm{e}}N_{\mathrm{b}}^2)$ in the occupied states functionals.

The minimization of the conventional energy functionals in terms of the DM or electronic orbitals requires an important intermediate step: in both cases the minimization has to be carried out with respect to variables satisfying some constraints. In the case of the orbital formulation, the wave functions need to be orthonormal

$$\langle\psi_i|\psi_j\rangle = \delta_{ij}, \tag{23}$$

whereas the density operator has to be idempotent (since it is the projection operator onto the occupied subspace) and normalized to the correct number of electrons:

$$\hat{\rho} = \hat{\rho}^2, \tag{24}$$

$$N_{\mathrm{e}} = \mathrm{Tr}(\hat{\rho}). \tag{25}$$

The conventional minimization procedure is performed in two steps: first, the gradient of the energy with respect to ψ_i or $\rho^{\mu\nu}$ is computed, and the variables are moved in the direction of these gradients; secondly, the constraints are imposed on new values of the variables. Imposing the orthonormality or idempotency constraints is in general an over-linear operation, even if the system is described in terms of Wannier functions [42], or truncated density matrices. Kohn proposed a method [43] to obtain truncated GWF applying a local Lowdin orthogonalization procedure coupled with an energy minimization. Therefore, in order to obtain variational methods which overcome the $\mathcal{O}(N^3)$ scaling, it is not sufficient to use the electronic localization properties, and one also needs to construct energy functionals which do not require to impose the constraints explicitly, or than handle them in such a way that the linear scaling is preserved. The development of such functionals has received much attention in the last few years, as will be described in Section 3.2.

3.2. New energy functionals

Several functionals, which do not require explicitly imposing the constraints, have been developed in the last few years. The functionals should have the correct minimum (i.e., the correct ground state energy), even if the variables of minimization are not forced to satisfy the constraints. A clear example of this kind of functionals is given in the orbital approach: the band structure energy Eq. (22) is the trace of the Hamiltonian in the occupied space. This trace can also be computed if the states ψ_i are nonorthogonal, in which case the correct expression involves the inverse of the overlap matrix between the electronic states: $S_{ij} = \langle\psi_i|\psi_j\rangle$

$$E_{\mathrm{BS}} = \mathrm{Tr}'(\hat{H}) = \sum_{ij}^{N} S_{ij}^{-1}H_{ji}, \tag{26}$$

where the prime in the trace indicates that it is taken on the occupied subspace, and $H_{ij} = \langle\psi_i|\hat{H}|\psi_j\rangle$. The unconstrained minimization of this functional with respect to ψ_i yields the cor-

rect ground state energy. At the minimum, the solutions do not need to be orthonormal, but the energy is the correct one. If the wave functions are orthogonalized, the energy would coincide with that of Eq. (22), since the overlap would be the unit matrix. This reflects the fact that the trace is a property of the subspace, and not of the basis that is used to compute it (either orthonormal or not). Another consequence of the invariance of the trace is that eigenvectors are not necessary to compute the energy, since any other combination of the occupied states would produce the same value. In particular, GWF can be used. Similarly, the density matrix can be evaluated using the nonorthogonal states and the inverse overlap matrix

$$\hat{\rho} = 2\sum_{ij}^{N} |\psi_i\rangle S_{ij}^{-1} \langle\psi_j| \tag{27}$$

and the representation in real space

$$\rho(\mathbf{r},\mathbf{r}') = 2\sum_{ij}^{N} S_{ij}^{-1} \psi_i(\mathbf{r})\psi_j(\mathbf{r}'). \tag{28}$$

The functional of Eq. (26) has indeed been used in electronic-structure calculations [44,45] in context of Galli and Parrinello [7] who used it in the first proposal of Order-N functional methods. They proposed the minimization of the energy functional in Eq. (26) with respect to *localized* wave functions which are nonzero only within certain localization region around their center, with radius R_c. These wave functions were expanded in terms of PW. Although the use of a PW basis makes the calculation difficult to carry out in practice (specially in imposing the localization constraints and in making the procedure to be scaled linearly, because of the delocalized character of PW), Galli and Parrinello showed a path that has been subsequently explored by several groups using localized basis sets. One of the difficulties of the functional in Eq. (26) is that, although no orthonormalization is required, one has to calculate the inverse of the overlap matrix S^{-1}, of dimension $N \times N$, which is a $\mathcal{O}(N^3)$ operation. In the work of Galli and Parrinello this was only a small part of the calculation, compared with those involving the PW basis, of size $N_b \gg N$. However, in TB approaches, it would require a significant amount of time, in fact quire similar to the one required by a diagonalization of the full Hamiltonian $\hat{H}$. Therefore, other functionals have been developed in which S^{-1} does not appear.

The first few forms of the functionals which were proposed to avoid the problem of the explicit constraints and the calculation of S^{-1} were cast either in the language of the DM, such as the methods proposed by Li et al. (LNV) [46] and Daw [47], or in terms of orbitals, such as the local orbital (LO) method developed independently by Mauri et al. [48] and Ordejón et al. [49]. However, it soon became apparent that both kinds of energy functionals could be expressed in the language of the DM [50,42]. In fact, it was later shown that they belong to a common, broader class of functionals that has been developed further by different authors. We will describe here this general formulation, and will give the details of the LNV and LO methods in the next few sections.

Hernandez et al. [9,10] developed a scheme that has later served to classify many of the different functionals developed in the last few years. The assumption of Hernandez et al. is that the DM in real space is representable in the form

$$\rho(\mathbf{r},\mathbf{r}') = \sum_{\alpha\beta}^{M} L^{\alpha\beta} \varphi_\alpha(\mathbf{r})\varphi_\beta(\mathbf{r}'), \tag{29}$$

where $\varphi_\alpha(\mathbf{r})$ are called "support functions" and are in general overlapping orbitals. M is the number of these support functions, and is equal or larger than the number of occupied states $N = N_e/2$. Note that the assumption in Eq. (29) is quite plausible. For instance, in an LCAO formulation the DM in real space takes exactly that form, with $\varphi_\alpha(\mathbf{r})$ being the basis functions (atomic orbitals), and $L^{\alpha\beta}$ the representation of the DM operator in the dual basis

$$\rho^{\alpha\beta} = \langle\varphi^\alpha|\hat{\rho}|\varphi^\beta\rangle = 2\sum_{i=1}^{N} C_{i\alpha} C_{j\beta}. \tag{30}$$

Eq. (29) can be however more general, since support functions might be themselves expressed in terms of a basis set, in which case Eq. (29) represents an assumption on the form of the DM. This latter approach was followed by Hernandez et al. in their Order-N scheme [9,10].

In order to avoid imposing explicitly the constraints on the DM, the functionals are constructed not in terms of the *trial* density matrix $\rho(\mathbf{r},\mathbf{r}')$, but in terms of a *purified* density matrix $\tilde{\rho}(\mathbf{r},\mathbf{r}')$. If the transformation from ρ to $\tilde{\rho}$ is properly chosen, the purified DM will be more idempotent than the trial DM. The purified DM is also assumed representable as

$$\tilde{\rho}(\mathbf{r},\mathbf{r}') = \sum_{\alpha\beta}^{M} K^{\alpha\beta}\varphi_{\alpha}(\mathbf{r})\varphi_{\beta}(\mathbf{r}'), \tag{31}$$

where the relation between K and L defines the purification transformation.

As shown by Galli in a recent review [51], a whole class of energy functionals can be defined by the above purification transformation. The energy is given by

$$\tilde{E}_{\mathrm{BS}} = \sum_{\alpha\beta}^{M} K^{\alpha\beta}\langle\varphi_{\alpha}|\hat{H}-\eta|\varphi_{\beta}\rangle + \eta N_{\mathrm{e}}. \tag{32}$$

The differences among functionals consist of the different choices of the transformation between L and K, the meaning of variable η and of the support functions and the number of them M. Galli has given a complete classification of the functionals in terms of these variables [51].

3.3. The Li–Nunes–Vanderbilt method

Li et al. [46] developed an energy functional based on the DM, which falls in the general class described in the former section. Daw [47] developed a closely related scheme, based in evolving the DM in temperature from $T=\infty$ to $T=0$. In the original implementation, the method was formulated in the context of orthogonal TB. Subsequent work by Nunes and Vanderbilt [52] and Ordejón et al. [42] generalized the functional to nonorthogonal basis sets. This more general formulation is the one we describe here.

3.3.1. The LNV functional

In the LNV method, the functional equation (32) is defined as follows. The support functions are simply the basis set orbitals ϕ_{μ}, and therefore their number is $M = N_{\mathrm{b}}$. In this case, the matrix L corresponds to the contravariant elements of the DM: $\rho^{\mu\nu}$, which are the variational parameters of the minimization. The purification transformation corresponds to the McWeeny transformation [53]

$$\hat{\tilde{\rho}} = 3\hat{\rho}^2 - 2\hat{\rho}^3. \tag{33}$$

The matrix K, which corresponds to the contravariant representation of $\hat{\tilde{\rho}}$, is given by

$$\mathbf{K} = 3\mathbf{LSL} - 2\mathbf{LSLSLSL} \tag{34}$$

(where $\mathbf{K}$ and $\mathbf{L}$ are the matrices $K^{\mu\nu} = \langle\phi^{\mu}|\hat{\tilde{\rho}}|\phi^{\nu}\rangle$ and $L^{\mu\nu} = \langle\phi^{\mu}|\hat{\rho}|\phi^{\nu}\rangle$). The parameter η corresponds in this case to the chemical potential μ (or Fermi level, since the calculations are done at $T=0$). The LNV functional therefore takes the form

$$\tilde{E}_{\mathrm{BS}} = \mathrm{tr}[\mathbf{K}(\mathbf{H}-\mu\mathbf{S})] + \mu N_{\mathrm{e}}, \tag{35}$$

where tr is the trace of the product of matrices (which has to be distinguished from the trace of the operators, denoted by Tr). The interpretation of the functional is quite straightforward [46,42]. We first note that the Hamiltonian is shifted by the chemical potential μ. Doing this is equivalent to working with the grand potential $\Omega = E - \mu N_{\mathrm{e}} = \mathrm{Tr}(\hat{\rho}(\hat{H}-\mu))$, which ensures that the normalization condition Eq. (25) will be satisfied at the solution. This is so because, after the energy shift, the occupied states (below the Fermi level) have negative energy, and their occupation will be maximized, whereas the empty states (above the Fermi level) have positive energy, and their occupation will be minimized. The position of the chemical potential must therefore be adjusted a priori or during the minimization, so that it lies within the energy gap, using the condition

$$N_{\mathrm{e}} = \mathrm{tr}(\mathbf{KS}) = \sum_{\mu\nu}^{N_{\mathrm{b}}} K^{\mu\nu}S_{\mu\nu}. \tag{36}$$

To see how the idempotency constraint is satisfied as the minimization proceeds, we notice that, if the functional is freely minimized with respect to K (i.e., without using the construction from L), the eigenvalues of $\tilde{\rho}$ corresponding to states below μ would be driven to $+\infty$, and those corresponding to states above μ would evolve to $-\infty$, and the energy would decrease indefinitely. However, if $\tilde{\rho}$ is

constructed from ρ by the purification transformation, the eigenvalues of $\tilde{\rho}$ are automatically restricted to the interval [0,1], since the function $f(x) = 3x^2 - 2x^3$ has a minimum at $f(0) = 0$, and a maximum at $f(1) = 1$ (see figure 1 in Ref. [46]). Eigenvalues of $\tilde{\rho}$ with negative energy will evolve to $+1$ and those with positive energy to 0, and therefore $\tilde{\rho}$ will be driven to idempotency *at the solution* of the minimization, without imposing idempotency explicitly.

It is clear, however, that the minimization procedure has *runaway solutions*, since the eigenvalues of $\tilde{\rho}$ can be outside the [0,1] interval if those of ρ are outside [–0.5, 1.5]. The physical minimum is therefore a *local*, and not a *global* one. In practice, this does not represent a problem, and the local minimum is reached without difficulty if the initial guess in the minimization process is chosen reasonably (the usual choice is a diagonal L matrix, with 0.5 in the diagonal [46]). We also note that an alternative derivation of the LNV functional, without any reference to the McWeeny purification transformation, was given by Ordejón et al. [42], in terms of Lagrange multipliers for the idempotency constraints.

In the practical implementation of the method, the energy functional Eq. (35) is minimized with respect to the values of $L^{\mu\nu}$. This minimization can be done by standard techniques like steepest descents or conjugate gradients (CG), since the energy gradients with respect to the degrees of freedom are readily calculated

$$\frac{\delta\tilde{E}}{\delta\mathbf{L}} = 3(\mathbf{SLH}' + \mathbf{H}'\mathbf{LS}) - 2(\mathbf{SLSLH}' + \mathbf{SLH}'\mathbf{LS} + \mathbf{H}'\mathbf{LSLS}) \quad (37)$$

(where $\mathbf{H}' = \mathbf{H} - \mu\mathbf{S}$ is the shifted Hamiltonian). The minimization is done along the line given by the gradient (or the conjugate gradient, in the CG approach). The line minimization can be done exactly, since the functional is a polynomial of third order in the parameter defining the line. It should be noted here that White et al. [54] have recently shown that the gradients in Eq. (37) are not tensorially consistent for the case of nonorthogonal bases, and have proposed an alternative form which satisfies the correct tensor properties. This gradients provide a more efficient minimization in the case of strongly nonorthogonal bases, but with the complication that it involves the S^{-1} matrix.

The calculations can be performed at constant chemical potential μ, which in MD simulations can yield to a variation of the total number of electrons by Eq. (36) (since the position of μ can change with the movement of the atoms). One can also fix the number of electrons, and adjust μ during the simulation. Qiu et al. [50] discussed a procedure to perform this adjustment efficiently, during the minimization of the energy functional.

The calculation of forces within the LNV scheme is also straightforward, as analytical derivatives of the energy functional. In general, the derivatives of $\tilde{E}$ with respect to a parameter λ (like, for instance, an atomic coordinate) is given by

$$\frac{\mathrm{d}\tilde{E}}{\mathrm{d}\lambda} = \mathrm{Tr}\left[\mathbf{L}\frac{d\mathbf{H}'}{\mathrm{d}\lambda}\right] + \mathrm{tr}\left[\mathbf{KH}'\mathbf{K}(3 - 4\mathbf{SK})\frac{\mathrm{d}\mathbf{S}}{\mathrm{d}\lambda}\right]. \quad (38)$$

An important extension of the LNV method has been done by Hernandez et al. [9,10], who used the concept of support functions discussed above to produce an ab-initio technique (within DFT) with Order-N scaling. They introduce the value of the support functions $\varphi_\mu(\mathbf{r})$ at the points of a real-space grid as additional variables in the energy functional, besides the matrix L. The minimization of the energy therefore produces the simultaneous optimization of the DM and the support functions. This real-space grid approach shows a lot of potential [55] because it is not biased by the choice of a particular basis set as in LCAO approaches. The drawback is that the cost is significantly larger, since the number of variables (value of each support function at each point of the grid) is very large.

We finally note that Corkill and Ho [56] have proposed a method to include fractional occupancy of electronic states in the LNV formalism, which allows to perform calculations with a finite electronic temperature. The method consists in using the Mermin free energy [57] $\Omega = E - TS$, with an appropriate polynomial approximation for the entropy S. Carlsson [58] has also used the LNV formulation together with a particular repre-

sentation of the trial density matrix in terms of "traveling" basis orbitals.

3.3.2. Localized density matrices

The elimination of the need to explicitly impose the normalization and idempotency constraints in the energy functional is the first step to achieve a linear scaling. The second one is to use the localization properties of the DM. Since the DM (either in real space $\rho(\mathbf{r},\mathbf{r}')$ or in the matrix representation L decays with the distance exponentially for insulators and as a power law for metals, a good approximation to the exact solution can be obtained by restricting the minimization to *strictly localized* DMs. This is done by searching for the minimum over DMs such that

$$L^{\mu\nu} = \langle \phi^{\mu} | \tilde{\rho} | \phi^{\nu} \rangle = 0 \quad \text{if } |\mathbf{R}_{\mu} - \mathbf{R}_{\nu}| > R_{\mathrm{c}}, \tag{39}$$

where $\mathbf{R}_{\mu}$ is the position of the atom in which the orbital ϕ_{μ} is centered. R_{c} is a real-space cutoff radius which depends on the decay properties of the DM for each particular system, and on the desired accuracy of the calculation, but not on the size of the system. If this truncation of the DM is imposed, the calculations necessary to evaluate the energy functional equation (35) scale as $\mathcal{O}(N)$. Indeed, if L is truncated at distances larger than R_{c} it will be a sparse matrix and the number of nonzero elements in each row (or column) will be small, and independent of the size of the system. The Hamiltonian and overlap matrices H and S are also sparse in a local orbital representation. The calculation of K and $\tilde{E}$ involve products of these sparse matrices. If the system is large enough, in each of the products, a new sparse matrix results (although with a longer range in real space than the matrices entering in the product). Since each product takes a computational effort proportional to the size of the system, the calculation of $\tilde{E}$ is an Order-N operation.

Since the energy functional is variational, the minimization of the functional with respect to truncated DMs yields an energy which is always higher or equal to the exact energy: for a given localization range R_{c}, we obtain a *variational upper bound* to the exact energy: $\tilde{E} \geqslant E_{\mathrm{exact}}$. For larger values of the localization range R_{c}, the variational freedom increases, and therefore the energy converges monotonically to the exact one with $R_{\mathrm{c}} : \tilde{E} \to E_{\mathrm{exact}}$ as $R_{\mathrm{c}} \to \infty$.

Fig. 4 shows the linear scaling of the method, for an MD simulation of diamond cells with different numbers of atoms, done with the ETB model of Ref. [59]. The crossover with the standard diagonalization is achieved for about 60 atoms in this particular case (although that depends critically on the value of R_{c} chosen, the range of the Hamiltonian model and the degree of packing of the system). It should be noted here that the application of the LNV formulation to nonorthogonal Hamiltonians is considerably more expensive than for orthogonal cases. This is due to the form of the purification transformation, in which the overlap matrix between basis orbitals S enters multiplying the trial density matrix L. This makes the resulting matrix product less sparse, with the consequent increase of the computational cost. Therefore, the sizes of systems for which the LNV formulation is faster than the standard diagonalization techniques are much larger for nonorthogonal Hamiltonians than for orthogonal ones. This problem does not arise in the case of the orbital formulations presented in the Section 3.4.

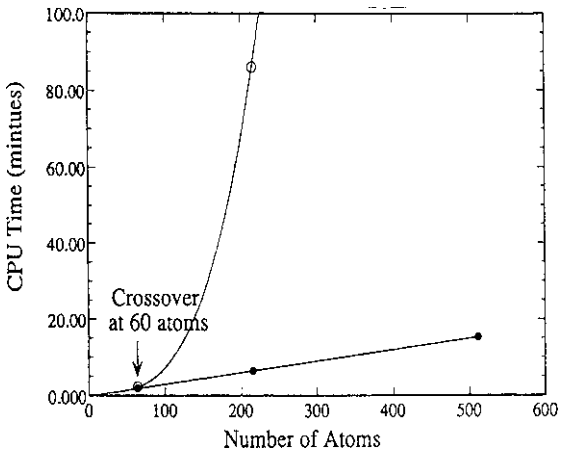

Fig. 4. . Comparison of the CPU for the LNV method (full circles) and the direct diagonalization (open circles) for 10 MD steps in crystalline carbon, for cells with different numbers of atoms. The calculations were done using an ETB model with first neighbor interactions; taken from Ref. [50].

3.3.3. Accuracy and applications

The LNV method has been tested in a variety of systems by different authors. Li et al. [46] have tested the convergence of the calculated physical properties with the cutoff R_c for a ETB model of crystalline Si. Fig. 5 shows the relative error in several physical quantities as a function of R_c. The error in the energy decreases monotonically as corresponds to a variational calculation. Other properties also converge to the exact value, but showing some oscillations. In general, errors smaller than 2% are achieved in all properties with the inclusion of the fifth shell of neighbors. An important consequence of imposing localization on the DM and that is clearly seen in Fig. 5, is that, at the solution, the number of electrons computed by means of Eq. (36) is not the exact one. However, it converges very quickly to the correct value.

The localization range R_c to achieve a given accuracy depends on the degree of localization of the DM. This depends on whether the system is metallic or an insulator, and on the value of the energy gap. This point is illustrated in Fig. 6, which shows the cohesive energies of several phases of carbon, versus the nearest-neighbor distance. All the results were obtained including a similar number of atoms in the localization regions (about 45), and

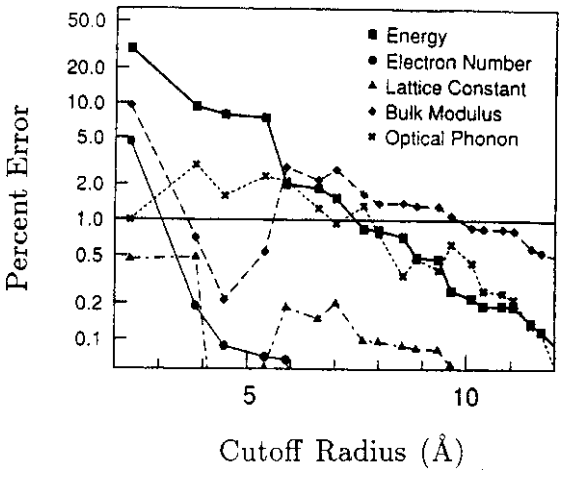

Fig. 5. Relative error (in percent) of the LNV density matrix method versus the localization range of the DM R_c. Results are for Si in the diamond structure, and were obtained using an empirical orthogonal TB model; taken from Ref. [46].

are compared with the exact diagonalization result. It is clearly seen that the accuracy for metallic phases is much poorer than for diamond and graphite (even if this later has a vanishing gap), reflecting the fact that the DM is less localized for metallic systems. Similar conclusions were drawn by Bowler and coworkers [60] in a recent comparative study between different Order-N schemes. The LNV method performed very well compared to other linear scaling methods for nonmetallic systems, whereas for metallic systems, recursion related approaches would be preferred (see, for instance, figures 9 and 10 of Ref. [60]).

The LNV method has been extensively applied to MD simulations. An important advantage of the method is that, at any level of truncation R_c, the forces are analytic derivatives of the approximate energy $\tilde{E}$, and therefore the quality of the generated MD trajectories is preserved. This is not true for other nonvariational methods, which show discrepancies between the forces and the derivatives of the computed forces, making it difficult to perform high quality MD simulations. This point has been thoroughly discussed by Bowler et al. in their comparative study. Another point, of course, is how the forces converge to the exact result as a function of R_c. This was also studied by Bowler et al., showing similar conclusions as for the cohesive energies. Qiu et al. [50] have done extensive tests on the quality of the MD trajectories for different crystalline, amorphous and liquid carbon systems. These tests show that the LNV method with truncated DM provides trajectories with a good energy conservation, and which follow closely those obtained with exact diagonalization. They have also discussed possible schemes to optimize the extrapolation of the DM between different time steps.

Vanderbilt and coworkers [61–63] have applied the LNV method to the study of dislocations in silicon. The possibility of studying systems with sizes up to 10^3 is essential in dealing with such extended defects in materials, allowing the determination of formation energies, migration barriers and kink-solition reaction pathways. Morris et al. [64] have studied the structure and energetics of tilt grain boundaries. They considered boundaries with different angles. For small angles the calculation re-

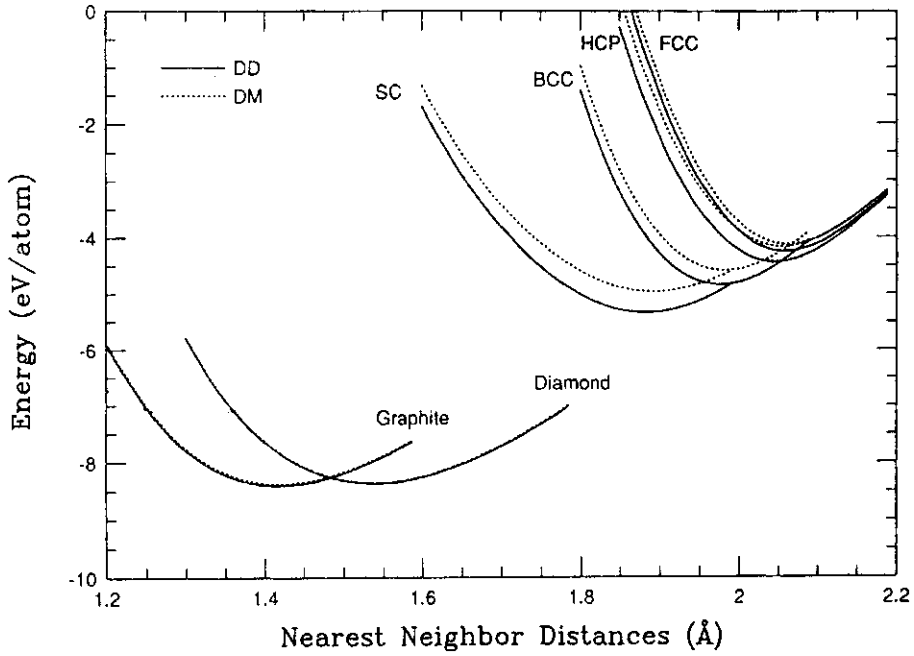

Fig. 6. Cohesive energy versus nearest-neighbor distance for different carbon structure. Full and broken curves are the results from exact diagonalization calculations and for the LNV density matrix approach, respectively; taken from Ref. [50].

quires several thousand atoms, due to the large periodicity, which is only possible with an Order-N. Kahn and Lu [65] also applied the LNV scheme to the calculation of structural properties and vibrational modes in silicon calthrates. The study of the structure and vibrations of large, complex systems is also a natural ground for application of these approaches.

Goringe et al. [66] have implemented the method of Hernandez et al. in parallel machines, obtaining excellent performances with systems containing several thousands of atoms. It should be noted, however, than the parallelization of these methods is more difficult than in the projection technique of Goedecker, since more information needs to be passed between processors in the matrix multiplications during the functional minimizations.

3.4. The local orbitals methods

The method of Localized Orbitals (LO) was first introduced independently by Mauri et al. [48] and by Ordejón et al. [49]. As in the case of the LNV functional, the idea was to derive a functional which, when minimized, would lead to the correct ground state energy, but for which the constraints would not need to be explicitly imposed. In the LO formulation, the variables of the functional minimization are the coefficients $C_{\mu i}$ of the expansion of the wave functions in an atomic orbitals basis (Eq. (11)). The derivations of Mauri et al. and Ordejón et al. are quite different. The first authors start with the functional of Eq. (26), which is valid for nonorthogonal states, and derive a new functional form by substituting the inverse overlap matrix by a truncated polynomial expansion in terms of powers of $(1-S)$. Ordejón et al., however, derive the same family of functionals by considering the form Eq. (22), which is only valid for orthonormal states, and introduce the constraints *within the functional* by means of a Lagrange multipliers term. A first approximation to the Lagrange multipliers yields the functional originally derived by Ordejón et al. which corresponds to the first order in the polynomial expansion of

Mauri et al. As was later shown by Ordejón et al. [42], successive approximations to the Lagrange multipliers yield the same family of functionals as those generated by the different polynomial approximations of the inverse overlap matrix in the derivation of Mauri et al.

3.4.1. The family of orbital energy functionals

The successive approximations to the inverse overlap matrix or to the Lagrange multipliers yield a family of functionals that can be expressed as

$$\tilde{E}^{(\mathcal{N})}[\chi] = 2\sum_{ij}^{N} Q_{ij}(H_{ji} - \eta S_{ji}) + \eta N_{\mathrm{e}}, \tag{40}$$

where $\chi_i = \sum_\mu C_{\mu i}\phi_\mu$ are the wave functions which are the variables of the minimization, $H_{ij} = \langle\chi_i|\hat{H}|\chi_j\rangle, S_{ij} = \langle\chi_i|\chi_j\rangle$, and

$$\mathbf{Q} = \sum_{n=0}^{\mathcal{N}} (\mathbf{I} - \mathbf{S})^n. \tag{41}$$

Different functionals are obtained with different orders $\mathcal{N}$ in the expansion of $\mathbf{Q}$. We will refer to these as the Mauri–Ordejón functionals. It can be shown [67,42] that, if $\mathcal{N}$ is an odd integer, and the constant η is such that the shifted Hamiltonian $(\hat{H} - \eta)$ is negative definite in the space spanned by the basis set $\{\psi_\mu\}$, then the energy functional $\tilde{E}^{(\mathcal{N})}$ has two important properties: (i) the *global* minimum with respect to the wave functions (or the coefficients $C_{\mu i}$) is the correct ground state energy, and (ii) the wave functions are orthogonal at the minimum: $S_{ij} = \delta_{ij}$. Therefore, an *unconstrained* minimization of the energy functional will yield the correct energy and an orthogonal solution. Note that no orthogonality constraints need to be explicitly imposed, and that orthogonality will only be achieved at the end of the minimization.

The charge density of the system can be computed consistently with the energy functional. According to Eq. (27) and with the approximation of S^{-1}, a the DM in real space will be given by

$$\tilde{\rho}(\mathbf{r}, \mathbf{r}') = 2\sum_{ij}^{N} Q_{ij}\chi_i(\mathbf{r})\chi_j(\mathbf{r}'). \tag{42}$$

It is easy to show that this corresponds to a purification transformation from the *trial* DM

$$\rho(\mathbf{r}, \mathbf{r}') = 2\sum_{i}^{N} \chi_i(\mathbf{r})\chi_i(\mathbf{r}'). \tag{43}$$

In terms of operators, we have

$$\hat{\tilde{\rho}} = \hat{\rho}\sum_{n=0}^{\mathcal{N}} (1 - \hat{\rho})^n. \tag{44}$$

Therefore, the Mauri–Ordejón functionals belong to the general class of functionals introduced in Section 3.2. Eq. (40) can be expressed in the form of Eq. (32). In this case, $\mathbf{L} = \mathbf{I}$ is fixed, $\mathbf{K} = \mathbf{Q}, \varphi$ are the wave functions χ, and $M = N = N_{\mathrm{e}}/2$.

The energy functionals of Eq. (40) only have a *global* minimum if the spectrum of the shifted Hamiltonian is negative. Since calculations are done with a finite basis set, this is always possible choosing an appropriate value for η. However, this is not necessary in practice, and a weaker condition can be imposed on η. It was shown [67,42] that the functionals have a *local* minimum if η is chosen to be larger than the highest occupied eigenvalue of $\hat{H}$. Therefore, there are runaway solutions, like in the LNV functional, but this does not cause problems in practice.

In practical applications, it is common to use the lowest order $(\mathcal{N} = 1)$ functional, for which $\mathbf{Q} = 2\mathbf{I} - \mathbf{S}$. This minimizes the number of matrix products, and yields the same correct energy when no localization constraints are imposed on the wave functions χ_i. We will discuss in the next section what the consequences of imposing localization are.

The minimization of the Mauri–Ordejón functional follows the same lines of the LNV method. The gradients of the energy functional with respect to the degrees of freedom (the coefficients $C_{\mu i}$, and the energy is minimized along the line defined by the gradients. The explicit formulas for the gradients as well as details on how to perform the line minimization can be found in Ref. [42].

The calculation of the forces is done by analytical derivation of the energy functional with respect to the atomic positions. The resulting expressions are given by Ordejón et al. in Ref. [42], in terms of the derivatives of the Hamiltonian

and overlap matrix elements in the atomic orbitals basis, as in the LNV case.

A generalization of the Mauri–Ordejón functionals was suggested by Kim et al. [68]. The idea is to use a number M of wave functions χ_i larger than the number of occupied states $N = N_e/2$, while keeping the same functional form. The energy functional and DM take the same form as in Eqs. (40) and (42), but the sum now runs over the M wave functions. The properties of the Kim's functional are the same as those of that of Mauri–Ordejón, except that the correct ground state energy is now obtained only if the value of η is within the gap between the highest occupied molecular orbital (HOMO) and the lowest unoccupied molecular orbital (LUMO). Since the number of wave functions is larger than the number of occupied states, η serves now to select which levels will be occupied or empty. One consequence is that the minimum is always local, and there is no global minimum. The minimization is nevertheless stable, unless the energy gap is too small, in which case some problems with runaway solutions may appear. Yang [69] has recently proposed a further generalization of this kind of functionals, for which there is an absolute global minimum, and that may have better stability properties in troublesome cases.

We should note that the family of Mauri–Ordejón functionals yield solutions that are orthogonal, so that the final overlap matrix is the unit matrix. For the Kim's case, however, the solution can be reached for a set of orbitals that *do* overlap. It can be shown that the overlap is such that N eigenvalues of the matrix S_{ij} have value equal to one, and the other $M - N$ are zero. Therefore, the solution is equivalent (by a unitary transformation) to N orthonormal wave functions and $M - N$ orbitals with zero norm [68].

In the same line as the orbital functionals described so far, Hierse and Stechel [70] have explored the possibility of using different forms of the relation between the wave functions χ_i and the trial DM. Instead of using the simple choice of $\mathbf{L} = \mathbf{I}$, they have proposed to use a more general expression of the form Eq. (29) (with $\varphi = \chi$), and use $\mathbf{L}$ as variational parameters, besides the wave functions. They choose to use the same number of wave functions as the number of occupied states ($M = N$). The advantage of such a formulation is that the wave functions χ_i that minimize the energy functional can be nonorthogonal. This can have favorable consequences when electronic localization is imposed, since nonorthogonal Wannier functions are more localized than orthogonal ones [71].

In contrast with the LNV method, the orbital methods presented in this section are well suited to the application in the context of nonorthogonal TB Hamiltonians. The overlap of the basis is naturally included, and the numerical effort is not significantly increased with respect to orthogonal bases. Nonorthogonal bases are inescapable for AITB calculations, and therefore the possibility of handling the overlap without a significant increase of the required effort is an important property of LO methods. Ordejón and coworkers [11,12,16] have developed an ab-initio LCAO scheme with linear scaling, using the LO approach. The method allows calculations with arbitrarily complete atomic basis sets, and within different fully self-consistent functionals of DFT (both within the local density approximation and with the inclusion of gradient corrections).

3.4.2. Localized orbitals

Once we have a series of functionals which can be minimized without any explicit implementation of the orthogonality constraints or the inversion of the overlap matrix, we introduce the second ingredient to achieve an Order-N scaling: the localization of the electronic states. In this case, the minimization of the functionals is done with respect to a set of *spatially truncated* wave functions χ_i. Each of these LO is restricted to be nonzero only in an appropriate region of space, which we call the localization region (LR). The LO is allowed to vary freely within the LR, in order to minimize the energy functional. The LO resulting in the energy minimization procedure will therefore resemble the generalized Wannier functions described in Section 2.2, but truncated besides some real-space cutoff. In an LCAO approach, the localization is easy to impose: a given LO χ_i centered at position $\mathbf{R}$ will be expanded only as a

function of the atomic orbitals ϕ_μ whose center $\mathbf{R}_\mu$ is closer than R_c:

$$\chi_i = \sum_{\mu}^{N_b} C_{\mu i}\phi_\mu, \qquad C_{\mu i} = 0 \quad \text{if } |\mathbf{R}_i - \mathbf{R}_\mu| > R_c. \tag{45}$$

Once the localization has been imposed, the method automatically scales as $\mathcal{O}(N)$, since, as in the case of the LNV functional, all the matrices become sparse.

The localization constraints would not introduce any error in the energy if the LO could be obtained as a unitary transformation of the occupied eigenfunctions. However, since the Wannier functions contain tails which decay but are not strictly zero, the truncation within the LR will produce certain errors in the computed energy. The localization approximation will be expected to work better for insulators than for metals, since the Wannier functions are exponentially localized.

An important feature in the present LO functionals is that the errors produced by the truncation of the LO are always positive, because the energy is variational. This is essential for the reliability of the method. It has been recognized [42,72] that in a nonvariational calculation with the standard functionals (Eq. (22) or Eq. (26)), the truncation of the LO within the LR produces large, uncontrolled errors in the computed total energy. The errors come from the approximate orthonormalization procedure necessary to apply the functional of Eq. (22), or in the calculation of the truncated S^{-1} matrix entering in the functional of Eq. (26). The variational character of the new energy functionals is essential to maintain the errors under control. Again, as in the case of the LNV functional, the calculated energy monotonically converges to the exact value when R_c is increased. For infinite localization range, the functional energy is exact.

The localization imposed on the wave functions has some effect in the behavior of the energy functional. For the Mauri–Ordejón and Kim's functionals, the solution is no longer completely orthogonal for the first case and with 0 or 1 eigenvalues of the overlap matrix for the second case. There is a slight deviation, which is stronger for shorter localization ranges. In consequence, similarly to the LNV case, the computed number of electrons at the solution is not the exact one, although it approaches it rapidly when the localization range is increased. This is also the case for the functional of Hierse and Stechel.

A main effect of the localization in the Mauri–Ordejón functional is that it introduces a multitude of local minima in the functional. The minimization is therefore significantly more difficult, since the procedure can be trapped in one of these local minima. This problem is severe if the minimization is started from a random initial guess. If, however, some physical information is used to initiate the minimization, the procedure converges to a better final solution (although there still are many local minima with very similar energy). One such way [42] is to build initial wave functions from bonding combinations of atomic orbitals. This approach was taken successfully in the applications presented in Refs. [73,74]. However, in cases where high disorder is present, this is not possible and the local minima produce severe problems. These local minima are also the cause that the energy conservation is poor during MD simulations [67,42]). Ordejón and coworkers [42] have studied strategies to improve the conservation of the energy and the quality of the trajectories during MD runs.

The problem of local minima was solved by the introduction of the functional of Kim et al. [68]. They showed that including a number of functions larger than the number of occupied levels eliminated the existence of local minima, and the dependence of the final solution on the initial guess (see figures 2 and 3 in Ref. [68]. The use of this functional is therefore recommended in cases where it is not possible to use physical information to build the initial wave functions.

In Fig. 7 we show the CPU time required by the LO scheme with the functional of Kim, compared to standard diagonalization. The results were obtained with the ab-initio LCAO method or Ordejón and coworkers [11,12,16], for a fully self-consistent LDA calculation for different Si supercells in the diamond structure. A minimal SZ basis was used in the calculation. The figure shows the CPU time per MD step in a dynamical simulation

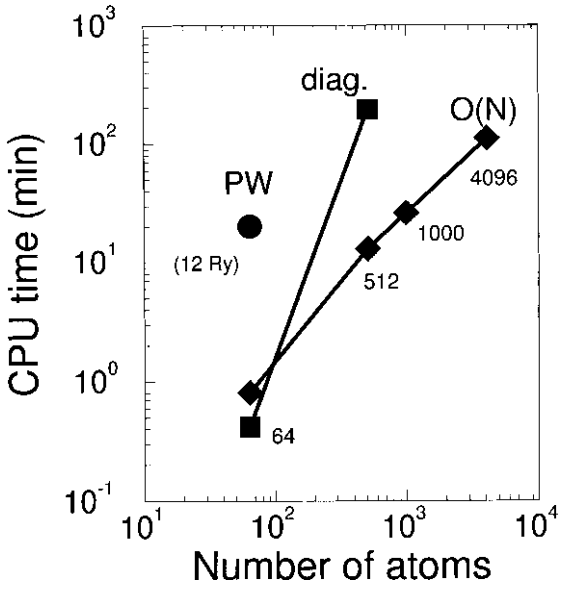

Fig. 7. Comparison of the CPU per MD time step with the LO functional of Kim and the direct diagonalization method. The results are obtained with the ab-initio LCAO method of Ordejón and coworkers. The point labeled PW denotes the typical CPU time required in a PW calculation in the same system.

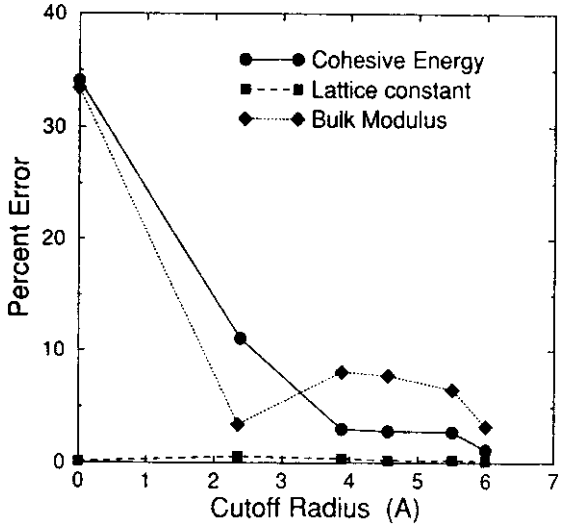

Fig. 8. Relative error (in percent) of the LO method of Mauri–Ordejón versus the localization range of the LR R_c. Results are for Si in the diamond structure, and were obtained using an the ab-initio TB model of Sankey and Nikleski; taken from Ref. [42].

done with an average temperature of 200 K. For comparison, we also show the typical CPU requirements of a PW calculation for the same system. We see that the $(\mathcal{O}(N)$ solution is faster than the standard diagonalization for relatively small system sizes, and that the present ab initio LCAO approach performs several orders of magnitude faster than PW calculations, at the cost of introducing some errors due to the small size of the LCAO basis set used.

3.4.3. Accuracy and applications

Ref. [42] shows several examples of the accuracy of the Mauri–Ordejón functional for the calculation of total energies, lattice constants, bulk moduli, phonons and MD simulations for silicon and carbon. Fig. 8 shows the accuracy of several properties for silicon in the diamond structure, as a function of the LR cutoff R_c. The results were obtained with the ab-initio Harris functional TB Hamiltonian of Sankey and Niklewski [75]. In this calculation, the center of the LR was chosen in the middle of the bonds between Si atoms. Each localized function includes all the atomic orbitals of atoms which are closer than R_c to either of the two atoms forming the bond. The convergence properties are quite similar to those of the LNV functional (Fig. 5). Small relative errors are obtained as soon as the third shell of neighbors are included in the LR, and with the fifth shell the errors are decreased below 3%. We note that in this calculation, the Hamiltonian and overlap between atomic orbitals extends up to the third shell of neighbors. This does not seem to have any effect on the quality of the solution in terms of localized orbitals.

The use of the functional of Kim improves the variational estimate of the energy for a given R_c, as shown in Table III of Ref. [68]. The reason is that the number LO is larger than in the Mauri–Ordejón functional, increasing the variational freedom. However, it requires the knowledge of the position of the chemical potential, which has to be determined during the calculation as in the LNV approach.

The functional of Hierse and Stechel gives a more accurate value of the energy than the other functionals, for a given localization range (see Table II in Ref. [70]. The reason is that nonorthogo-

nal Wannier functions are more localized than orthogonal ones, and therefore the truncation has a less strict effect in the computed energy. This, however, is achieved at the cost of introducing a larger number of minimization variables, through the matrix **L**, which is kept constant in the Mauri–Ordejón and Kim's functionals. As discussed by Hierse and Stechel [70], the most attractive feature of their functional is that the solution is more transferable than the orthogonal solution, since orthogonality between neighbor local orbitals means some degree of mixture that makes them less transferable between different environments.

The Mauri–Ordejón and Kim's functionals have been thoroughly applied to MD simulations. The properties of the generated dynamics were analyzed by several papers [67,42,68].

The application of the present functionals to metals has been very scarce. The reason is the slow decay of the Wannier functions in metals. Mauri and Galli performed an MD simulation of liquid-C, obtaining quite good results, even though it is a metallic system. However, the metallic character is quite special, and the electronic states are localized because of disorder. For normal metals with delocalized states, the performance of the method is not satisfactory.

Many practical applications of these functionals have been presented since they were proposed. Lewis and coworkers [73,74] have used the Mauri–Ordejón functional for the study of large biological molecules. They studied for the first time the structure, electronic and vibrational states of a DNA helix using electronic-structure methods [73]. The segment contained a whole turn of the helix, with a total of 644 atoms. Galli and coworkers [76–78] have done extensive studies of the deposition of C_{60} and C_{28} fullerenes on semiconductor surfaces, and the formation of films of amorphous solids during the deposition. The calculations were done using the functional of Kim, by MD simulations of the impact of the fullerenes on the surface, which reveals the process of formation of the thin film. Kim et al. [79] studied the structure of extended {3 1 1} defects in silicon, Itoh et al. [80,81] presented a study of the structure and energetics of giant fullerenes, and its evolution with size.

The LO method has also been parallelized by various groups [82,83], with results similar to those obtained with the DM approaches. Again, the main difficulty arises in the need to share information between processors in the matrix multiplications.

3.5. Functionals based on penalty functions

Two functional forms have been proposed in the literature which do not fit in the classification scheme discussed so far. In these functionals, the constraints are not forced by a purification transformation which changes the functional form in different ways depending on the choice of the transformation and the variables. Instead, a penalty function is added to the total energy functional. The penalty is a positive function that increases with the deviation from the constraints, and therefore forces the minimization toward a solution that satisfies them.

The method of Wang and Teter [84] is based on an orbital approach, in which a penalty function is added to the total energy of Eq. (22) to force the wave functions towards orthogonality. The functional takes then the form

$$\Omega[\psi] = 2\sum_{i}^{N}\langle\psi_i|\hat{H}|\psi_i\rangle + \lambda\sum_{ij}^{N}|\langle\psi_i|\psi_j\rangle|^2, \tag{46}$$

where λ is a constant which has to be large enough so that the penalty wins over the possible decrease in the first term which can derive from nonorthogonal solutions. Wang and Teter have analyzed how the results can be affected by the choice of λ.

Kohn [6] has recently proposed a functional based on the DM that also uses a penalty function to achieve the constraints (in this case, the idempotency of the DM). The total energy functional takes the form

$$\Omega[\tilde{\rho}] = E[\tilde{\rho}^2] - \mu N[\tilde{\rho}^2] + \alpha P[\tilde{\rho}] + \mu N_e, \tag{47}$$

where $\tilde{\rho}$ is the trial DM, μ, the chemical potential, $E[\tilde{\rho}^2]$, the standard energy functional evaluated with the square of the trial DM, $N[\tilde{\rho}^2]$, the total number of electrons resulting from the square of the trial DM, and P, the following penalty function:

$$P[\tilde{\rho}] = \left[\int \mathrm{d}\mathbf{r}\, \tilde{\rho}^2 (1-\tilde{\rho})^2 |_{\mathbf{r}'=\mathbf{r}} \right]^{1/2}. \quad (48)$$

The penalty is zero if the DM is idempotent, and positive otherwise. The normalization of the DM to the corrected number of electrons is achieved by the chemical potential as in the LNV case. The last term (μN_e) is a constant shift to compute the energy from the grand potential $\Omega = E - \mu N$. Kohn has shown that, for a given chemical potential μ, if α is larger than a certain critical value α_c, the unconstrained minimization of the functional provides the exact ground state energy. At the solution, the trial DM is idempotent. The value of α_c is of the order of the spectral width of the occupied levels times $N(\mu)^{1/2}$.

To date there have been no applications of these two functionals to large scale systems, and therefore we will not discuss them further.

3.6. Focusing of small parts of large systems

Ordejón et al. [85] presented a method to compute the dynamical matrix and the phonons of large systems from electronic-structure calculations, with an effort proportional to the number of atoms. The method was implemented with the local orbital scheme of Mauri–Ordejón, but could be adapted to any of the functionals presented above. The idea is to compute the change in the total energy with the displacement of a given atom by allowing to change only those LO which are near the atom that is moving. This will yield the dynamical matrix elements coupling that atom with the rest, and is an $\mathcal{O}(1)$ operation. The calculation of the whole dynamical matrix will therefore be proportional to the number of atoms in the system. The method was applied to determine the vibrational spectra of giant fullerenes with up to 3840 atoms.

This approach points to a possible use of linear scaling techniques based on electronic localization which has not been much explored. It would consist on focusing on local parts of a large system, like in local relaxations, chemical reactions in large molecules, surface problems, etc. The calculation would concentrate on the electronic variables near the region of interest, producing an algorithm that would scale as the size of that region, and not of the whole system. The electronic variables in other regions would be maintained fixed, providing an optimal boundary condition for the part of interest. The advantage of this scheme in conjunction with the variational energy functionals is that the local optimization is easy to do in terms of only a few variables (those included in the region of interest), and the energy is still variational (an upper bound to the exact energy). Therefore, the errors are kept under control, and will diminish if the region in which the variables are allowed to change is large enough.

4. Projection methods

The Projection Methods (PM) are another alternative for the computation of total energies and forces in large systems with an Order-N scaling. The basic idea of these methods is to use an approximation to the DM to compute the energy by means of Eq. (10). The calculation is not variational, and it therefore does not involve a minimization. The DM (which, at $T=0$ is the projector operator into the occupied subspace) is approximated by a polynomial expansion in terms of powers of the Hamiltonian. In order to achieve linear scaling, the localization properties of the DM are again invoked.

In Section 4.1 we will discuss the method to approximate the Fermi–Dirac projection operator. In Section 4.2 we discuss the PM as applied to the calculation of the total energies and forces, whereas in Section 4.3 we describe recent proposals for other uses of the PM, like obtaining generalized Wannier functions, and providing general proofs of the localization of the DM.

4.1. Chebyshev expansion of the Fermi–Dirac projector

In order to calculate the Fermi–Dirac projector operator or DM in Eq. (1), it is approximated by a polynomial expansion in terms of the Hamiltonian. Sankey et al. [86] proposed to make the expansion in terms of Chebyshev polynomials, which provide an optimal representation in the minimax

sense (minimal largest error in the interpolation interval, for a given polynomial order). Other authors have also used the same Chebyshev expansion [87–90,29], which has to be done at a finite temperature, to avoid the discontinuous behavior of the Fermi–Dirac function. Since the Chebyshev polynomials provide an interpolation in the interval [–1, 1], we first need to shift and scale the Hamiltonian so that its eigenvalues are within that interval. The Fermi–Dirac function is therefore approximated by a polynomial of degree N_{pl}

$$\hat{F}_{\mathrm{pl}}(\hat{H}) = \frac{c_0}{2} + \sum_{j=1}^{N_{\mathrm{pl}}} c_j T_j(\hat{H}), \tag{49}$$

where the coefficients c_i, which depend on the chemical potential μ and the inverse temperature β, are calculated numerically [91]. The Chebyshev polynomials satisfy recursion relations that are of utility:

$$T_0(\hat{H}) = \hat{I}, \tag{50}$$

$$T_1(\hat{H}) = \hat{H}, \tag{51}$$

$$T_{j+1}(\hat{H}) = 2\hat{H}T_j(\hat{H}) - T_{j-1}(\hat{H}). \tag{52}$$

We note that these are equalities between operators. The expressions as matrices in a basis set depend on the orthogonality or nonorthogonality of the basis. In what follows, we will assume that the basis is orthogonal, although the formulation for nonorthogonal bases has been described by Baer and Head-Gordon [29] and by Stephan and Drabold [90].

The projection method can be considered as a moments method. The Fermi operator is described as a polynomial series of powers of the Hamiltonian. These are just the moments of $\hat{H}$, as will be seen in Section 5.1. Unlike other moments based methods, the projection technique does not relay on the spectral information (density of states, Green's functions, etc.), but it serves to compute the energy in a direct way, as we describe in Section 4.2.

Let us now discuss the choice of the inverse temperature β and the order of the polynomial expansion N_{pl}. Calculations usually aim at the zero temperature properties of the system, and therefore a large enough value of β should be chosen. However, the Fermi–Dirac distribution varies more abruptly with increasing β, a higher order polynomials would be required to represent it accurately. However, if the system has a gap $\delta\epsilon$ this is fortunately not needed: one can chose β in such a way that the Fermi–Dirac distribution only changes appreciably from the zero temperature value at energies within the energy gap. The smooth variation within the gap does not have any effect on the computed properties, since no states are present at those energies. Once β has been chosen with this criterion, the order of the polynomial is chosen so as to represent the resulting Fermi–Dirac function accurately. Goedecker has given an estimate of $N_{\mathrm{pl}} \approx 4(\epsilon_{\max} - \epsilon_{\min})/\delta\epsilon$. If the system is metallic, β is the physical inverse temperature, and the result of the calculation will be sensitive to its value. For calculations of metals at low temperature, a high value of β will be required, which will imply a higher order polynomial and the consequent increase of the calculation cost.

4.2. The projection method for total energies and forces

Sankey et al. [86] developed a scheme that used the above polynomial expansion, combined with random vectors and recursion, to determine the occupied eigenstates of the Hamiltonian. Total energies and forces are therefore available from the knowledge of the occupied states. The scaling of the method was still cubic with the size of the system, and therefore we will not discuss it further here.

The full potential of the projection technique for Order-N calculations was uncovered by Goedecker and coworkers [87,88]. These authors have used the Chebyshev expansion of Eq. (49) to evaluate the total energy given by Eq. (10). If the last equation is expressed in terms of an orthogonal basis of localized atomic orbitals ϕ_μ, one obtains Eq. (13), in which the matrix elements of the Fermi–Dirac operator between basis set vectors appear. However, since the DM is localized in real space, these matrix elements will be small for dis-

tant orbitals. As an approximation, as in the previous section, they can be neglected beyond certain localization region LR defined by a radius R_c, leading to an Order-N scaling. The details of the procedure are as follows. We define the wave functions f_μ which result from applying the Fermi–Dirac operator on each atomic orbital ϕ_μ. The energy can be expressed as

$$E = \sum_{\mu}^{N_b} \langle \phi_\mu | \hat{H} | f_\mu \rangle. \tag{53}$$

Using the Chebyshev expansion for $\hat{F}$, we have

$$|f_\mu\rangle = \hat{F}|\phi_\mu\rangle \approx \hat{F}_{pl}(\hat{H})|\phi_\mu\rangle = \frac{c_0}{2}|t_\mu^0\rangle + \sum_{j=1}^{N_{pl}} c_j |t_\mu^j\rangle, \tag{54}$$

where the functions $|t_\mu^j\rangle$ are computed using the recursion relations:

$$|t_\mu^0\rangle = |\phi_\mu\rangle,$$

$$|t_\mu^1\rangle = \hat{H}|\phi_\mu\rangle,$$

$$|t_\mu^{j+1}\rangle = 2\hat{H}|t_\mu^j\rangle - |t_\mu^{j-1}\rangle, \tag{55}$$

$|f_\mu\rangle$ corresponds to a column of the Fermi–Dirac matrix, and therefore will show exponential or power law localization in insulators and metals, respectively. This is illustrated in Fig. 9 for the cases of carbon and aluminum. The slower decay in Al is clearly observed.

Truncation within R_c is now imposed. To achieve that, and since $|f_\mu\rangle$ is computed by applying the Hamiltonian successively on the vectors $|t_\mu^j\rangle$, Goedecker propose to apply "reflecting" boundary conditions: whenever such a multiplication of H by a vector is done, the resulting vector is truncated within R_c. In this way, the calculation of each of the vectors f_μ is an $\mathcal{O}(1)$ operation, and the calculation of the energy scales linearly with the number of orbitals, and therefore with the number of atoms.

A great advantage of the present formulation is that the calculation of each of the vectors f_μ is independent of all the others, which makes the method very easy to parallelize [87]. A disadvantage, on the other hand, is that, in MD simulations, a given time step can not use any information of the solution of the previous time steps, as can be done in the functional methods. The solution has to be computed from scratch.

The forces can be obtained as derivatives of the polynomial expansion, and the explicit formulas are given by Goedecker et al. [87,88]. We stress that the formulation presented here is only valid

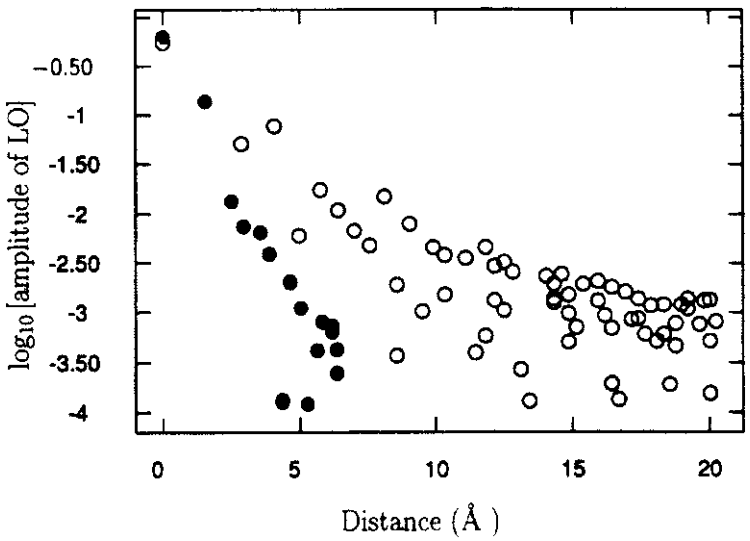

Fig. 9. Decay of the projected orbitals f_μ in C (full circles) and Al (open circles); taken from Ref. [88].

for orthogonal bases. The nonorthogonal case is considerably more complicated [29,90], since involves the inverse of the overlap matrix between atomic orbitals. Interested readers are referred to Ref. [90] for details on how to solve the inverse overlap matrix problem in an Order-N way.

Goedecker and Teter [88] have analyzed the accuracy and the performance of the method in MD simulations with empirical TB Hamiltonians. Fig. 10 shows the absolute error in the total energies and forces for crystalline carbon. Both quantities converge rapidly to the exact value with the localization range R_c. They find that, although the method is not variational, the quality of the forces is satisfactory for MD simulations. They have applied the method to liquid-C, obtaining similar results to those of Mauri and Galli with the variational LO method [67].

Stephan and Drabold [90] have made a careful analysis of the possible sources of error in the projection method: (i) the use of a finite value for β, (ii) the truncation of the Chebyshev expansion, (iii) the use of a finite R_c and (iv) the approximations involved in the calculation of the inverse overlap matrix in the nonorthogonal formulation. They give explicit formulas to estimate these errors, and conclude that, at least for insulators, the most crucial parameter is the localization R_c of the orbitals: for reasonable values of β and N_{pl}, the choice of R_c determines the accuracy of the calculation. They also show that the convergence of the energy with R_c is not monotonic, in contrast with the variational schemes. This indicates that careful convergence tests are needed for specific applications.

4.3. Other applications: Generalized Wannier functions and localization theorems

Besides providing an efficient Order-N technique for computing total energies and forces, the projection method also can be used to obtain generalized Wannier functions. These can be useful for a variety of applications, like the calculation of polarization and effective charges (see, for instance, the discussions in Refs. [27,92], and references therein). They can also be used as an optimal initial guess for the variational LO methods described in Section 3.4. Stephan and coworkers [90,93] have explored this approach.

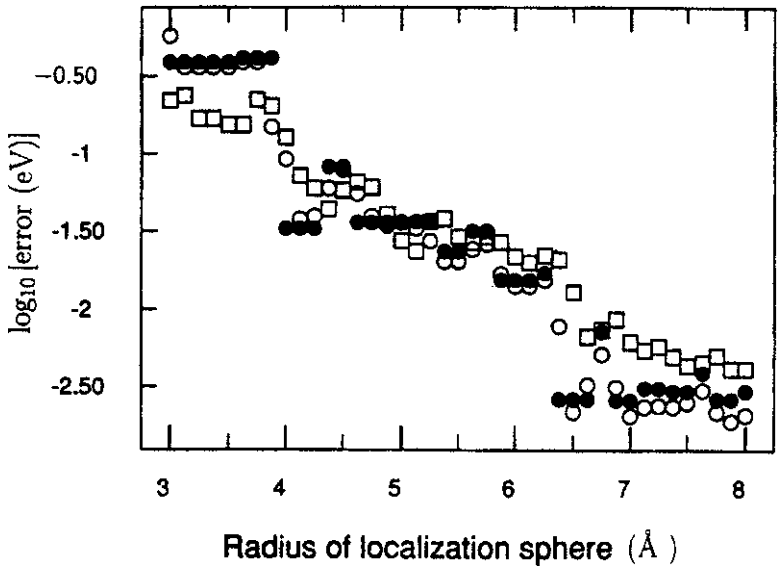

Fig. 10. Results of projection method of Goedecker for carbon, as a function of the localization range R_c. Full circles show the error in the total energy (in eV), for an ordered diamond structure; open circles show the same quantity for a slightly randomly disordered diamond crystal; squares show the relative error of the forces for the same disordered crystal; taken from Ref. [88].

The orbitals f_μ obtained by applying the Fermi–Dirac operator over a given atomic orbital ϕ_μ are localized functions which live in the occupied subspace (because of the projection, only the component within the occupied space survives). To obtain linearly independent functions, we therefore select the desired number of initial orbitals at random, and apply the projection operator on them. If the number of electrons is N_e, we will need $N = N_e/2$ such functions. The resulting localized states, however, will be highly nonorthogonal. In order to obtain the orthogonal generalized Wannier functions, an orthogonalization procedure is required. Stephan and Drabold [90] describe possible ways of achieving this, preserving the linear scaling.

Another application of the projection technique has been explored by Baer and Head-Gordon [29,30]. Since the degree of the polynomial in the Fermi–Dirac expansion depends directly on the energy gap of the system, they have given arguments to show what are the localization properties of the DM as a function of the gap for insulating systems, and as a function of the electronic temperature for metals. The conclusions seem to be of general validity, and serve as a general proof of localization in electronic systems.

5. Spectral methods

In this section we will describe methods that are intended to provide information about the spectrum of the Hamiltonian, or that use this information to compute other properties like total energies, forces, etc. These methods are complementary to those described in the previous sections, which are very well suited for total energy and forces calculations but do not provide any spectral information. Many properties of interest in materials depend on the spectrum, and therefore methods which provide such information are of very high value.

In contrast to total energy approaches, which only have flourished in the last decade after the ideas of Car–Parrinello, spectral methods have a very long tradition in electronic-structure calculations. Green's functions have been used to compute electronic properties since many decades. They provide a natural form to describe the electronic states in terms of the local environment, and have therefore been widely applied to systems with broken periodicity [94] like defects [95], surfaces [20], amorphous solids [21], etc.

We do not intend to provide here a detailed overview of the subject, and we will restrict ourselves to describing in general terms those recent approaches that intend to solve the electronic-structure problem of systems with large number of atoms with an Order-N effort. We will first describe in Section 5.1 the general concepts involved in these methods. Section 5.2 treats different schemes to obtain approximate moments, and Section 5.3 describes ways to reconstruct the physical information from the moments. Finally, in Section 5.4 we will mention a method to obtain exact eigenvectors and eigenvalues at selected energies with an Order-N effort.

5.1. Moments of the density of states

The normalized density of states (DOS) of a system is an energy dependent quantity defined by the following equation:

$$n(\epsilon) = \frac{1}{N_b}\sum_{i=1}^{N_b}\delta(\epsilon - \epsilon_i), \tag{56}$$

where N_b is the size of the basis, which is equal to the total number of eigenstates, and ϵ_i are the eigenvalues. The band structure energy can be expressed in terms of the DOS, as

$$E_{BS} = 2N_b\int^{\epsilon_F} \epsilon n(\epsilon)\ \mathrm{d}\epsilon. \tag{57}$$

The DOS is a *global* property of the system. It can, however, be decomposed into *local* densities of states (LDOS) [94] associated to the different basis orbitals ϕ_α

$$n(\epsilon) = \frac{1}{N_b}\sum_{\alpha}^{N_b} n_\alpha(\epsilon) \tag{58}$$

with

$$n_\alpha(\epsilon) = \sum_{i=1}^{N_b} |C_{\alpha i}|^2 \delta(\epsilon - \epsilon_i). \quad (59)$$

$C_{\alpha i}$ are the coefficients of the eigenstates in the basis (Eq. (11)). We have assumed that the basis set is orthonormal. The generalization of the moments methods to nonorthogonal bases is also possible (see, for instance, Ref. [96]), but we will not consider it here for simplicity. The DOS and the LDOS can be represented in terms of their moments. The pth moment of the LDOS n_α is defined as

$$\mu_\alpha^{(p)} = \int \epsilon^p n_\alpha(\epsilon)\, d\epsilon \quad (60)$$

with a similar definition for the moment of the total DOS. The moments can be expressed in a more useful way as powers of the Hamiltonian:

$$\mu_\alpha^{(p)} = \langle \phi_\alpha | \hat{H}^p | \phi_\alpha \rangle = \sum_{\beta_1 \beta_{2\ldots} \beta_{p-1}}^{N_b} H_{\alpha\beta_1} H_{\beta_1\beta_2} \ldots H_{\beta_{p-1}\alpha} \quad (61)$$

and, for the moments of the total DOS

$$\mu^{(p)} = \frac{1}{N_b} \sum_{\alpha}^{N_b} \langle \phi_\alpha | \hat{H}^p | \phi_\alpha \rangle = \frac{1}{N_b} \sum_{\beta_1 \beta_{2\ldots} \beta_p}^{N_b} H_{\beta_1\beta_2} H_{\beta_2\beta_3} \ldots H_{\beta_{p-1}\beta_p}. \quad (62)$$

The knowledge of a the moments up to a certain order should allowed us to reconstruct the DOS or LDOS, since the moments bear the information about the center, spectral range and shape of these functions. From the densities of states, one can obtain the rest of the physical properties. In the next few sections, we describe how to obtain *approximate* moments, and how to reconstruct the densities of states from them.

Eqs. (61) and (62) provide a clear picture of why moments based methods can easily be made to scale linearly with the size of the system. In both equations, a moment of order p is obtained by a process of hopping around the lattice along closed paths of length p. Therefore, to obtain a given moment, only a finite cluster is necessary. Truncation of the moment expansion to a given order means that only clusters up to a given size are required. Computing the LDOS of each orbital is therefore an $\mathcal{O}(1)$operation, provided that the system size is larger than the maximum cluster size. Therefore, obtaining the total DOS and the energy is an $\mathcal{O}(N)$ operation. The procedure can be further optimized in the following way: for a given order of the polynomial, one can restrict the hops to a cluster of a size smaller than the one that would be in principle required. This would allow only paths of p hops that remain close enough to the site under consideration, which will be more important than those exploring farther regions. This approach is very similar to the reflecting boundary conditions in the Hamiltonian multiplications of the Goedecker method described in Section 4.2.

5.2. Methods to obtain approximate moments

A large number of methods have been developed to obtain estimates of the moments. Here we review some of them, which have shown potential for application in large-scale calculations.

5.2.1. The Lanczos method

One of the most widely used methods to obtain information on the moments of the LDOS is the Lanczos recursion algorithm [97]. The moments are not obtained directly, although the computed quantities contain the same information. The method is an efficient scheme for tridiagonalizing a matrix. Given an initial state $|U_0\rangle$, a recursion relation is generated by successive application of the Hamiltonian:

$$\begin{aligned} \hat{H}|U_0\rangle &= a_0|U_0\rangle + b_1|U_1\rangle, \\ \hat{H}|U_1\rangle &= a_1|U_1\rangle + b_1|U_0\rangle + b_2|U_2\rangle, \\ &\vdots \\ \hat{H}|U_m\rangle &= a_m|U_m\rangle + b_m|U_{m-1}\rangle + b_{m+1}|U_{m+1}\rangle. \\ &\vdots \end{aligned} \quad (63)$$

The states $|U_m\rangle$ generated by the recursion series are orthonormal ($\langle U_m|U_n\rangle = \delta_{mn}$), and therefore the Hamiltonian, in the representation of those states, is tridiagonal. Starting from a known state $|U_0\rangle$, the recursion coefficients a_m and b_m are com-

puted using Eq. (64) successively and imposing normalization of the states. The procedure therefore provides with the series of states $|U_m\rangle$ and the recursion coefficients a_m and b_m.

If the initial state for the recursion is chosen to be one of the orbitals of the basis, let us say $|\phi_\alpha$, the recursion coefficients have a close relation with the moments of the LDOS $n_\alpha(\epsilon)$, by virtue of Eq. (61) and the completeness of the states $|U_m\rangle$:

$$\begin{aligned}
\mu_\alpha^{(0)} &= 1,\\
\mu_\alpha^{(1)} &= a_0,\\
\mu_\alpha^{(2)} &= a_0^2 + b_1^2,\\
\mu_\alpha^{(3)} &= a_0^3 + 2a_0 b_1^2 + a_1 b_1^2.\\
&\vdots
\end{aligned} \tag{64}$$

Therefore, carrying out the Lanczos recursion to an order m provides us with the first m moments of the LDOS, Note, however, that the inversion from recursion coefficients to moments can be numerically unstable. Therefore, in most common cases, the Lanczos scheme is used to obtain the recursion coefficients, which are then used directly to obtain the Green's functions and the density of states, as will be described in Section 5.3.1.

We note that the Lanczos method provides the exact recursion coefficients up to the order in which the recursion is carried out, unless approximations based on the truncation of the cluster over which the Hamiltonian hops are allowed are taken. In this case, the linear scaling is preserved, but errors are involved in the calculated recursion coefficients (see Ref. [60]).

5.2.2. The local truncation approach

Silver and coworkers [98–103] have developed a method to compute approximate moments of the LDOS in an Order-N way. The procedure follows quite closely the comments made at the end of Section 5.1, and is very much related to the D&C scheme of Yang [32] and the projection method of Goedecker [87]. The basic idea is to compute the moments of the LDOS for a given orbital by using Eq. (61), but restricting the Hamiltonian to a subspace containing only orbitals which are in a localization region around the orbital. The cost of the calculation of the moments of each orbitals is therefore independent of the size of the system, and therefore obtaining the moments for all the orbitals scales as $\mathcal{O}(N)$. In their work, they use Chebyshev moments instead of raw power moments, because they yield an algorithm numerically more stable

$$\mu_\alpha^{T_p} = \int_{-1}^{1} T_p(\bar{\epsilon}) n_\alpha(\bar{\epsilon})\ \mathrm{d}\bar{\epsilon}, \tag{65}$$

where $\bar{\epsilon}$ is the energy shifted and scaled so that the eigenvalues of the Hamiltonian are in the interval $[-1, 1]$. Once the approximated moments are computed, the density of states can be reconstructed with one of the methods of Section 5.3. Silver and coworkers have used this scheme in combination with different procedures for the reconstruction of the DOS. In Fig. 11 we show results of a calculation of the atomic relaxations in a vacancy in silicon [99]. The figure shows the convergence in the two different atomic distances originated by the Jahn–Teller distortion, as a function of the number of moments included in the calculation. The results were obtained imposing truncation beyond the third shell of neighbors. The difference

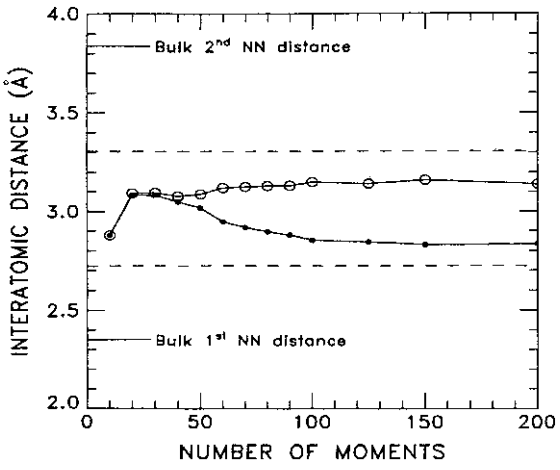

Fig. 11. Results for the structure of a vacancy in Silicon (the two different interatomic distances), obtained by the local truncation approach and the Kernel polynomial method (circles), as a function of the number of moments included. The dashed lines are the exact results. The residual error for large number of moments is the result of the local truncation; taken from Ref. [99].

between the Order-N result for high number of moments and the exact one (dashed lines) is due to this truncation.

5.2.3. The statistical approach

Skilling [104] noted the possibility of extracting moments from the operation of the Hamiltonian on random vectors, which Drabold and Sankey [105] developed further into an Order-N scheme. Somewhat related ideas where proposed by Varga [106], and used later by Krajc and Hafner [107] in another Order-N approach. Here we will describe the method of Drabold and Sankey.

We take a set of n_v random normalized states $|\xi_i\rangle$, from which we compute

$$v_i^{(p)} = \langle \xi_i | \hat{H}^p | \xi_i \rangle. \tag{66}$$

It is easy to see that, if a sufficiently large sampling of such random vectors is taken, then the average $\langle v^{(p)} \rangle$ coincides with the moments of the DOS $\mu^{(p)}$. The calculation of each of the $v_i^{(p)}$ scales as $\mathcal{O}(pN)$, if the Hamiltonian is sparse, since it involves p multiplications of $\hat{H}$ over a vector. The average therefore will be an $\mathcal{O}(pn_vN)$ operation. Drabold and Sankey have observed that the number of random vectors does not grow with the size of the system, and therefore computing the moments will be Order-N. Stephan et al. [93] have made an analysis to the relative errors, showing that, for isolated states in the DOS, they decrease with n_v, but do not depend on the system size, whereas for continuous DOS the errors decrease with both N_v and N. Therefore, for continuous features in the DOS, the method requires less random vectors for larger system sizes, and its scaling is therefore sublinear.

Random vectors were also used by Iitaka and coworkers [108,109] to calculate the linear response with an Order-N, together with a Chebyshev expansion of the projection operator. The method allows the calculation of the frequency dependent dielectric constants for very large systems, and was applied to hydrogenated silicon nanoclusters with 13 464 Si atoms. Wang [110] performed calculations in similar but smaller systems, with Chebyshev moments obtained from random vectors.

5.3. Reconstructing the density of states from approximate moments

Once that the moments of the DOS or LDOS have been obtained, a method is needed to reconstruct these functions, and compute the physical properties of the system. Although many possible schemes have been devised, only some of them are enough robust and stable to produce results with arbitrary accuracy. Many of the methods become unstable for large numbers of moments, and are therefore not well suited for precise calculations. Here we will describe briefly some of the methods that have proved successful.

5.3.1. Recursion methods

The method of recursion [5,22] is one of the most widely used to build the density of states from the moments. The method provides a stable representation of the DOS in terms of Green's functions, which is expressed as a continuous fraction. For a given state $|U_0\rangle$, the diagonal element of the Green's function can be expressed in terms of the recursion coefficients a_m and b_m generated by the Lanczos method from $|U_0\rangle$

$$G_{00}(Z) = \cfrac{1}{Z - a_0 - \cfrac{b_1^2}{Z - a_1 - \cfrac{b_2^2}{Z - a_2 - \cfrac{b_3^2}{\ddots}}}}. \tag{67}$$

The Green's function allows us to compute the local density of states on a particular orbital:

$$n_\alpha(\epsilon) = -\frac{1}{\pi} \lim_{\eta \to 0} \mathrm{Im}\{G_{\alpha\alpha}(\epsilon + \mathrm{i}\eta)\} \tag{68}$$

from which the total energy can be computed.

These relations are the basis of many approaches. One of them is the Bond-Order Potentials method [111,112], which has been recently reviewed by Horsfield and coworkers [113]. The method provides a natural link between electronic-structure and empirical classical potentials, and presents a series of nice features like the ability to compute accurate forces, which is a difficult issue in Green's functions based methods. The interested readers are referred to the work of Horsfield et al. [113], and a recent work by Bowler et al. [60] where the performance of the method for Order-N

calculations of total energies, forces and MD is presented, and compared with others. One of the main conclusions of that study is that the BOP method is preferred over other Order-N schemes like the LNV functional when metallic systems are studied.

Baroni and Giannozzi [114] developed a scheme based on the recursion formalism to compute the Green's function in real space without the use of orbitals. The method used a discretization of the Hamiltonian in the points of a grid in real space, and solved the Green's function by recursion. The truncation of the continuous fraction after a finite number of steps produces the linear scaling of the method.

The multiple scattering method [115] is also based on the use of Green's functions of a given atom, which are calculated taking into account only a number of shells around it. The method shows excellent potential for parallelization, and has shown to provide a quite accurate description of the energies of disordered phases of metal.

5.3.2. The maximum entropy method

The maximum entropy (Maxent) method [104] provides a way to reconstruct original data from incomplete information. This is exactly the kind of problem that one faces when trying to obtain the DOS from a finite number of moments, and therefore Maxent provides a possible solution. Several authors have tested this possibility [116–118,105,103,102] with satisfactory results. The details of Maxent algorithm can be found in [118]. In essence, the method tried to find the DOS $n(\epsilon)$ which satisfies the constraints that it must reproduce the values of the moments computed by some other method. The Maxent principle requires that the solution maximizes the "entropy"

$$S \equiv -\int n(\epsilon)\ \ln(n(\epsilon))\ \mathrm{d}\epsilon. \tag{69}$$

The method is stable with very large numbers of moments, so that considerable spectral resolution can be achieved (see figure 2 in Ref. [119], where van-Hove singularities are nicely described). In Fig. 12 shows the density of states computed with a Maxent reconstruction of the moments obtained

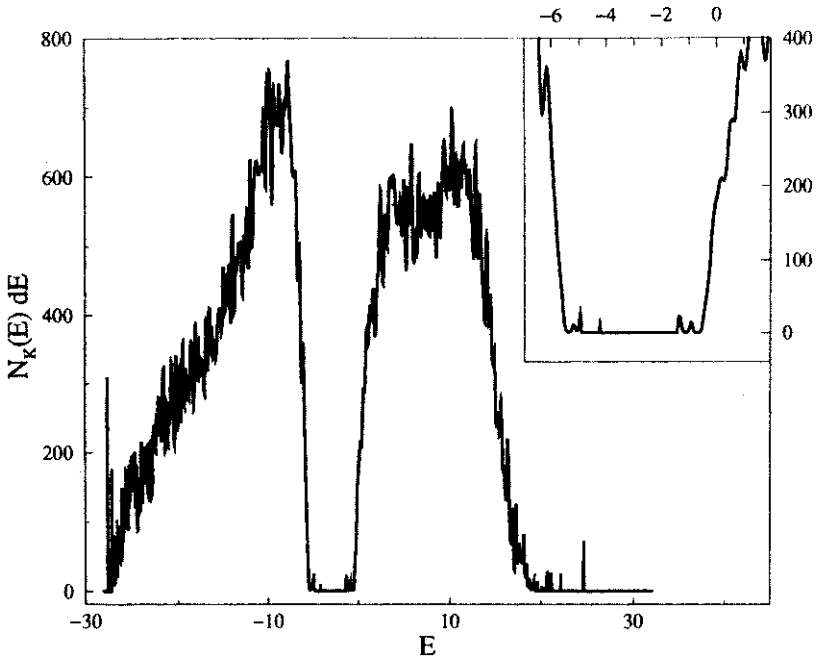

Fig. 12. Density of states of an amorphous carbon periodic cell with 4096 atoms; taken from Ref. [101].

by the statistical approach described of Section 5.2.3. The system is a 4096 atoms cell of amorphous carbon. The accuracy of the calculation depends in this case on the number of random vectors used to obtain the moments, and on the number of moments used in the reconstruction. In this case, a very large number (512) was used to reproduce the localized states within the energy gap. Smaller numbers of moments provide less resolution, since the amount of information for the reconstruction of the DOS is also smaller. Only four random vectors were used in the example shown. Dong and Drabold further applied the Maxent method with moments obtained from random vectors for the study of band tails in amorphous silicon and carbon [120,121].

5.3.3. The kernel polynomial method

In the Kernel Polynomial method (KPM) [98–103], the density of states is approximated by an expansion in terms of orthogonal polynomials. Chebyshev polynomials are the most common choice. Since only a limited number of moments are available, this is a truncated polynomial expansion, which shows typical Gibbs oscillation phenomena. These can be dumped with appropriate Gibbs factors g_p, so that the approximation to the density of states is given by

$$n(\epsilon) \approx \frac{1}{\pi\sqrt{1-\epsilon^2}}\left[\mu^{(T_0)} + 2\sum_{p=1}^{M}\mu^{(T_p)} g_p T_p(\epsilon)\right], \qquad (70)$$

where $\mu^{(T_p)}$ are the Chebyshev moments defined in Eq. (65), and M, the number of moments in the expansion. The optimal values of g_p can be found in Ref. [99]. It can be shown that the above estimate of the DOS is a convolution of the exact DOS with a Kernel polynomial. The width of the convolution function is smaller for larger orders M of the expansion, thus providing with higher spectral resolution.

5.4. The folded spectrum method

To conclude the description of spectral methods with Order-N scaling, we will briefly describe a methods that can be used to compute specific eigenstates and eigenvalues for large systems, with an effort proportional to the size of the system for each computed state. In contrast with the methods described so far, where the Order-N scaling is achieved at the cost of doing some approximations, this method is exact (but the cost of each state is $\mathcal{O}(N)$).

Several methods enable us to calculate the extremal eigenvalues of a sparse Hamiltonian in Order-N operations. One is the Lanczos method; another is the minimization or maximization of the expectation value of the Hamiltonian for all possible wave functions $|\psi\rangle$. However, the calculation of a state that is not at the extremes of the spectrum is problematic. The Lanczos procedure can be used to compute the second low-lying state once the first is known, by imposing orthogonality to it. However, the process is unstable as soon as a few levels have been obtained, due to the loss of orthogonality between the states in the Lanczos chain originated from finite-precision arithmetic [122].

A solution to this problem is the folded spectrum method, which seems to have been derived independently by several authors [123–128]. The central idea is that, if ψ_i is an eigenstate of $\hat{H}$ with eigenvector ϵ_i, then it will also be an eigenstate of $(\hat{H}-\epsilon_{\text{ref}})^2$, with eigenvalue $(\epsilon_i-\epsilon_{\text{ref}})^2$. This operator has the same eigenstates as $\hat{H}$, but its spectrum is folded about ϵ_{ref}. Therefore, the lowest eigenvalue of the folded operator can be obtained by Lanczos [128] or by minimization of $\langle\psi(\hat{H}-\epsilon_{\text{ref}})^2|\psi\rangle$ with respect to all possible wave functions [123,125], and this will provide us with the eigenstate and eigenvalue of the original Hamiltonian $\hat{H}$ closest to ϵ_{ref}. Hence, we can compute any eigenstate of the $\hat{H}$ which just choosing the reference energy ϵ_{ref}.

6. Conclusions

We have described a number of methods that allow us to solve the electronic problem of large systems with an effort which scales linearly with the number of atoms. The main physical idea behind these methods is the locality in the electronic structure, which different methods exploit in different manners. The development of these methods is

proceeding at a very high rate, and new methods and improvements on existing ones are continuously being proposed. With these techniques, we are now able to look into the possibility of studying problems which were out of the question a few years ago. The combination of these methods with the availability of fast workstations and with massively parallel computers can represent a revolution in the applicability and predictive power of electronic-structure methods in materials and biological systems.

An interesting effect of the appearance and development of Order-*N* techniques has been a renewed interest in the TB approach, both empirical and from first principles. TB provides an ideal framework to understand the properties of condensed matter systems from a local perspective. Since Order-*N* is based on locality, TB is the natural languages in which Order-*N* methods are formulated. Since larger systems sizes are being accessible, the interest in developing more accurate and reliable TB models is increasing.

So far, most of the Order-*N* methods have been developed and applied in the context of empirical or semiempirical model Hamiltonians. This is manly due to the fact that, in first principle approaches, the solution of a given Hamiltonian is only one aspect of the problem. The other side is the construction of that Hamiltonian from first principles. Doing so in Order-*N* operations is not an straightforward task. However, advances in that direction are also proceeding fast, and now there are some schemes that have solved this problem and allow us to perform ab-initio simulations with systems of thousands of atoms.

As has been often pointed out, as increasingly larger sizes are becoming available in our simulations, we start encountering another problem, which can represent an important barrier for future development. It is the issue of the simulation time. For large systems, the presence of slow degrees of freedom makes the time scale increase. For instance, changes in configurations in macromolecules, or propagations of cracks in materials are processes for which the time scale is unattainable for the present techniques. Advances in this field would be very much needed.

References

[1] P. Hohenberg, W. Kohn, Phys. Rev. 136 (1964) 864.
[2] R. Car, M. Parrinello, Phys. Rev. Lett. 55 (1985) 2471.
[3] M.C. Payne et al., Revs. Mod. Phys. 64 (1992) 1045.
[4] C.M. Goringe, D.R. Bowler, E. Hernandez, Rep. Prog. Phys. 60 (1997) 1447.
[5] V. Heine, in: F. Seitz, C. Turnbull, H. Ehrenreich (Eds.), Solid State Physics: Advances in Research and Applications, vol. 35, Academic Press, New York, 1980.
[6] W. Kohn, Phys. Rev. Lett. 76 (1996) 3168.
[7] G. Galli, M. Parrinello, Phys. Rev. Lett. 69 (1992) 3547.
[8] Y. Huang, D.J. Kouri, D.K. Hoffman, Chem. Phys. Lett. 243 (1985) 367.
[9] E. Hernandez, M.J. Gillan, Phys. Rev. B 51 (1995) 10157.
[10] E. Hernandez, M.J. Gillan, C.M. Goringe, Phys. Rev. B 53 (1996) 7147.
[11] P. Ordejón, E. Artacho, J.M. Soler, Phys. Rev. B 53 (1996) 10441.
[12] P. Ordejón, E. Artacho, J.M. Soler, Mat. Res. Soc. Symp. Proc. 408 (1996) 85.
[13] J.C. Burant, G.E. Scuseria, M.J. Fisch, J. Chem. Phys. 105 (1996) 8969.
[14] M.C. Strain, G.E. Scuseria, M.J. Frisch, Science 271 (1996) 51.
[15] J.M. Stratmann, G.E. Scuseria, Chem. Phys. Lett. 257 (1996) 216.
[16] D. Sanchez-Portal, P. Ordejón, E. Artacho, J.M. Soler, Int. J. of Quantum Chem. 65 (1997) 453.
[17] J.M. Pérez-Jordá, W. Yang, J. Chem. Phys. 107 (1997) 1218.
[18] G. Lippert, J. Hutter, M. Parrinello, Molecular Physics 92 (1997) 477.
[19] S. Goedecker, O.V. Ivanov, Solid State Commun. 105 (1998) 665.
[20] L.M. Falicov, F. Yndurain, J. Phys. C 8 (1975) 147.
[21] F. Yndurain, J.D. Joannopoulos, M.L. Cohen, L. Falicov, Solid State Commun. 15 (1974) 617.
[22] R. Haydock, V. Heine, M.J. Kelly, J. Phys. C: Solid State Phys. 5 (1972) 2845.
[23] G.H. Wannier, Phys. Rev. 52 (1937) 191.
[24] E.I. Blount, Solid State Phys. 13 (1962) 305.
[25] S.F. Boys, Rev. Mod. Phys. 32 (1960) 296.
[26] W. Kohn, Phys. Rev. 115 (1959) 809.
[27] N. Marzari, D. Vanderbilt, Phys. Rev. B 56 (1997) 12847.
[28] S. Goedecker, Preprint archive xxx.lanl.gov: Number: cond-mat/9804013, 1998.
[29] R. Baer, M. Head-Gordon, J. Chem. Phys 107 (1997) 10003.
[30] R. Baer, M. Head-Gordon, Phys. Rev. Lett. 79 (1997) 3962.
[31] S. Ismail-Beigi, T. Arias, Preprint archive xxx.lanl.gov: Number: cond-mat/9805147, 1998.
[32] W. Yang, Phys. Rev. Lett. 66 (1991) 1438.
[33] W. Yang, J. Mol. Str. (Theochem) 255 (1992) 461.
[34] S.L. Dixon, K.M. Merz, J. Chem. Phys. 104 (1996) 6643.

[35] T.-S. Lee, D.M. York, W. Yang, J. Chem. Phys. 105 (1996) 2744.
[36] E. Artacho, L.M. del Bosch, Phys. Rev. A 43 (1991) 5770.
[37] W. Yang, Phys. Rev. A 44 (1991) 7823.
[38] J. Harris, Phys. Rev. B 31 (1985) 1770.
[39] W. Yang, T.-S. Lee, J. Chem. Phys. 103 (1995) 5674.
[40] W. Zhao, W. Yang, J. Chem. Phys. 102 (1995) 9598.
[41] T. Zhu, W. Pan, W. Yang, Phys. Rev. B 53 (1996) 12713.
[42] P. Ordejón, D.A. Drabold, R.M. Martin, M.P. Grumbach, Phys. Rev. B 51 (1995) 1456.
[43] W. Kohn, Chem. Phys. Lett. 208 (1993) 167.
[44] I. Štich, R. Car, M. Parrinello, S. Baroni, Phys. Rev. B 39 (1989) 4997.
[45] T.A. Arias, M.C. Payne, J.D. Joannopoulos, Phys. Rev. Lett. 69 (1992) 1077.
[46] X.-P. Li, W. Nunes, D. Vanderbilt, Phys. Rev. B 47 (1993) 10891.
[47] M.S. Daw, Phys. Rev. B 47 (1993) 10895.
[48] F. Mauri, G. Galli, R. Car, Phys. Rev. B 47 (1993) 9973.
[49] P. Ordejón, D.A. Drabold, M.P. Grumbach, R.M. Martin, Phys Rev. B 48 (1993) 14646.
[50] S.-Y. Qiu, C. Z Wang, K.M. Ho, C.T. Chan, J. Phys.: Condens. Matter 6 (1994) 9153.
[51] G. Galli, Curr. Opin. Sol. State & Mater, Sci. 1 (1996) 864.
[52] R. Nunes, D. Vanderbilt, Phys. Rev. B 50 (1994) 17611.
[53] R. McWeeny, Rev. Mod. Phys. 32 (1960) 335.
[54] C.A. White, P. Maslen, M.S. Lee, M. Head-Gordon, Chem. Phys. Lett. 276 (1997) 133.
[55] E. Hernandez, M.J. Gillan, C.M. Goringe, Phys. Rev. B 55 (1997) 13485.
[56] J.L. Corkill, K.M. Ho, Phys. Rev. B 54 (1996) 5340.
[57] N.D. Mermin, Phys. Rev. 137 (1965) A1441.
[58] A. Carlsson, Phys. Rev. B 51 (1995) 13935.
[59] C.H. Xu, C.Z. Wang, C.T. Chan, K.M. Ho, J. Phys.: Cond Matt. 4 (1992) 6047.
[60] D.R. Bowler et al., Modelling Simul. Mater. Sci. Eng. 5 (1997) 199.
[61] R.W. Nunes, J. Bennetto, D. Vanderbilt, Phys. Rev. Lett. 77 (1996) 1516.
[62] J. Bennetto, R.W. Nunes, D. Vanderbilt, Phys. Rev. Lett. 79 (1998) 245.
[63] R.W. Nunes, J. Bennetto, D. Vanderbilt, Phys. Rev. 57 (1998) 10388.
[64] J.R. Morris, C.L. Fu, K.M. Ho, Phys. Rev. B 54 (1996) 132.
[65] D. Kahn, J.P. Lu, Phys. Rev. B 56 (1997) 13898.
[66] C.M. Goringe, E. Hernandez, M.J. Gillan, I.J. Bush, Comp. Phys. Commun. 102 (1997) 1.
[67] F. Mauri, G. Galli, Phys. Rev. B 50 (1994) 4316.
[68] J. Kim, F. Mauri, G. Galli, Phys. Rev. B 52 (1995) 1640.
[69] W. Yang, Phys. Rev. B 56 (1997) 9294.
[70] W. Hierse, E.B. Stechel, Phys. Rev. B 50 (1994) 17811.
[71] P.W. Anderson, Phys. Rev. Lett. 21 (1968) 13.
[72] K.C. Pandey, A.R. Williams, J.F. Janak, Phys. Rev. B 52 (1995) 14415.
[73] J.P. Lewis, P. Ordejón, O.F. Sankey, Phys. Rev. B 55 (1997) 6880.
[74] J.P. Lewis, N.H. Pawley, O.T. Sankey, J. Chem. Phys. B 101 (1997) 10576.
[75] O.F. Sankey, D.J. Niklewski, Phys. Rev. B 40 (1989) 3979.
[76] G. Galli, F. Mauri, Phys. Rev. Lett. 73 (1994) 3471.
[77] A. Canning, G. Galli, J. Kim, Phys. Rev. Lett. 78 (1997) 4442.
[78] J. Kim, G. Galli, J.W. Wilkins, A. Canning, J. Chem. Phys 108 (1998) 2631.
[79] J. Kim, J.W. Wilkins, F.S. Khan, A. Canning, Phys. Rev. B 55 (1997) 16186.
[80] S. Itoh, P. Ordejón, D.A. Drabold, R.M. Martin, Phys. Rev. B 53 (1996) 2132.
[81] S. Itoh et al., Sci. Rep. RITU A 41 (1996) 163.
[82] S. Itoh, P. Ordejón, R.M. Martin, Comp. Phys. Commun. 88 (1995) 173.
[83] A. Canning et al., Comp. Phys. Commun. 94 (1996) 89.
[84] L.-W. Wang, M.P. Teter, Phys. Rev. 46 (1992) 12798.
[85] P. Ordejón, D.A. Drabold, M.P. Grumbach, R.M. Martin, Phys. Rev. lett. 75 (1995) 1324.
[86] O.F. Sankey, D.A. Drabold, A. Gibson, Phys. Rev. B 50 (1994) 1376.
[87] S. Goedecker, L. Colombo, Phys. Rev. Lett. 73 (1994) 122.
[88] S. Goedecker, M. Teter, Phys. Rev. B 51 (1995) 9455.
[89] D.J. Kouri, Y. Huang, D.K. Hoffman, J. Phys. Chem. 96 (1996) 7903.
[90] U. Stephan, D.A. Drabold, Phys. Rev. B 57 (1998) 6391.
[91] W.H. Press, B.P. Flannery, S.A. Teukolsky, W.T. Vetterling, Numerical Recipes, Cambridge, New York, 1986.
[92] P. Fernandez, A. del Corso, F. Mauri, A. Baldereschi, Phys. Rev. B 55 (1997) 1909.
[93] U. Stephan, D.A. Drabold, R.M. Martin, to be published.
[94] J. Friedel, Adv. Phys. 3 (1954) 446.
[95] J. Bernholc, N.O. Lopari, S.T. Pantelides, Phys. Rev. B 21 (1980) 3545.
[96] A. Gibson, R. Haydock, J.P. LaFemina, Phys. Rev. B 47 (1993) 9229.
[97] C. Lanczos, J. Res. Natl. Bur. St. 45 (1950) 225.
[98] R.N. Silver, A.F. Voter, J.D. Kress, H. Roeder, in: A. Tentner (Eds.), Simulation MultiConference '95 Proceedings, High Performance Computing '95, The Society for Computer Simulations International, San Diego, CA, 1995.
[99] A.F. Voter, J.D. Kress, R.N. Silver, Phys. Rev. B 53 (1996) 12733.
[100] R.N. Silver, H. Roeder, A.F. Voter, J.D. Kress, J. Comp. Phys. 124 (1996) 115.
[101] H. Roeder et al., in: A. Tentner (Ed.), Simulation Multi-Conference '96 Proceedings, High Performance Computing '96, The Society for Computer Simulations International, San Diego, CA, 1996.
[102] H. Roeder, R.N. Silver, D. Drabold, J. Dong, Phys. Rev. B 55 (1997) 15382.
[103] R.N. Silver, H. Roeder, Phys. Rev. B 56 (1997) 4822.
[104] J. Skilling, in: J. Skilling (Ed.), Maximum Entropy and Bayesian Methods, Kluwer, Dordrecht, 1989.
[105] D.A. Drabold, O.F. Sankey, Phys. Rev. Lett. 70 (1993) 3631.

[106] S. Varga, J. Phys. Condens. Matter. 2 (1990) 8303.
[107] M. Krajc, J. Hafner, Phys. Rev. Lett. 74 (1995) 5100.
[108] T. Iitaka et al., Phys. Rev. E 56 (1997) 1222.
[109] S. Nomura et al., Phys. Rev. B 56 (1997) 4348.
[110] L.-W. Wang, Phys. Rev. B 49 (1994) 10154.
[111] D. Pettifor, Phys. Rev. Lett. 63 (1989) 2480.
[112] M. Aoki, Phys. Rev. Lett. 71 (1993) 3842.
[113] A. Horsfield et al., Phys. Rev. B 53 (1996) 12694.
[114] S. Baroni, P. Giannozzi, Europhys. Lett. 92 (1992) 547.
[115] Y. Wang et al., Phys. Rev. Lett. 75 (1995) 2867.
[116] L.R. Mead, N. Papanicolau, J. Math. Phys. 25 (1984) 2404.
[117] R.H. Brown, A.E. Carlsson, Phys. Rev. B 32 (1985) 6125.
[118] I. Turek, J. Phys. C 21 (1988) 3251.
[119] D.A. Drabold, P. Ordejón, J.J. Dong, R.M. Martin, Solid State Commun. 96 (1995) 833.
[120] J. Dong, D.A. Drabold, Phys. Rev. B 54 (1996) 10284.
[121] J. Dong, D.A. Drabold, Phys. Rev. Lett. 80 (1998) 1928.
[122] L.-W. Wang, A. Zunger, Comp. Mat. Sci. 94 (1994) 326.
[123] R.B. Capaz, G.C. de Araujo, B. Koiler, J.P. von der Weid, J. Appl. Phys 74 (1993) 5531.
[124] G. Grosso, L. Martinelli, G.P. Parravicini, Nuovo Cimento D 15 (1993) 269.
[125] L.-W. Wang, A. Zunger, J. Chem. Phys. 100 (1994) 2394.
[126] L.-W. Wang, A. Zunger, J. Phys. Chem. 98 (1994) 2158.
[127] B. Koiler, R.B. Capaz, Phys. Rev. Lett. 74 (1995) 769.
[128] G. Grosso, L. Martinelli, G.P. Parravicini, Phys. Rev. B 51 (1995) 13033.